SURFACE WAVE DISPERSION IN LAYERED ANISOTROPIC MEDIA

Thesis by

Don L. Anderson

In Partial Fulfillment of the Requirements

For the Degree of

Doctor of Philosophy

California Institute of Technology

Pasadena, California

1962

TABLE OF CONTENTS

ABSTRACT

An analysis is made of the dispersive properties of layered anisotropic media, emphasis being placed on the geophysically important case of transverse isotropy. Period equations are derived for Rayleigh, Stoneley and Love type waves. A correspondence is established, in certain cases, with ray theoretical and plane stress solutions.

The general anisotropic problem (orthorhombic symmetry) is considered briefly for certain propagation directions and is used to derive the two-dimensional theory of seismic modeling.

The single layer solutions are generalized to the n-layer problem by use of Thomson-Haskell matrices. The results are used to interpret long period surface wave data. It is found that an anisotropy of approximately 8% in the low velocity zone removes the discrepency between Love and Rayleigh waves.

ACKNOWLEDGMENTS

The author wishes to express his appreciation to Dr. Frank Press for his many helpful suggestions and encouragement throughout the course of this work. David G. Harkrider developed the multi-layered anisotropic Rayleigh program which considerably shortened the period between conception of theory and practical application.

During various periods of this research the author held National Science Foundation Fellowships and a Standard Oil Company of California Fellowship and this support is gratefully acknowledged.

Most of the computations were performed on the IBM 7090 computer at the Jet Propulsion Laboratory and the Burrough's 220 at the Caltech Computing Center.

The figures were prepared by Laszlo Lenches and the author wishes to extend special thanks to him for this assistance.

I. INTRODUCTION

The earth is generally assumed in both theory and practical application to be isotropic, or, at most, to be composed of plane parallel isotropic layers. While this assumption is made for mathematical convenience it probably holds true, at least approximately, for large portions of the earth. Certain discrepancies are being uncovered, however, by the continually increasing accuracy and range of our observations which indicate a need for a more general theory. The nature of some of these discrepancies suggests that they may be due to anisotropy. In addition to this indirect evidence, sufficiently detailed studies often demonstrate directly the presence of anisotropy. See, for example, White and Sengbush (1953), Jolly (1956), Uhrig and Van Melle (1955) and Layat et al. (1961). These results can usually be attributed to the presence of finely layered material, such as shale. Gassman (1951) has presented theoretical arguments for the existence of anisotropy in granular material. Non-uniform stress fields also generate directional elastic properties.

The direct manifestation of anisotropy is the directional dependence of wave velocity. Appropriate experiments can easily be performed in the lab but require a major effort in the field. In general we are limited to indirect evidence.

Some of the indirect manifestations of anisotropy are:

a) introduction of additional body phases

b) components of particle displacement non-orthogonal to the azmuthal coordinate system

c) coupling of body phases

d) displacement and distortion of surface wave dispersion curves

e) disagreement between Love and Rayleigh wave structures, computed on the basis of isotropic theory

f) distortion and tilting of surface wave particle motion orbits

g) coupling of Love and Rayleigh waves

h) splitting of resonance peaks

i) non-parallel directions of group and phase velocity

j) existence of cusps on wave-fronts.

The existence and degree of these phenomena depend on the nature of the anisotropy and the relation between the elastic constants.

Anisotropy is exhibited in its purest form in single crystals but can also occur in a collection of crystals or minerals which has crystallized or has been deposited with a preferred orientation, or has been subjected to non-uniform forces after formation. Layered media by their very nature are anisotropic in the large but the individual layers may also be anisotropic in a manner which cannot be handled by a further subdivision into finer layers. Heterogeneous media with random grain orientation tend to be isotropic.

Theoretical studies of anisotropy to date have dealt with limiting cases such as infinite wave length (Helbig, 1958; Postma, 1955; White and Angona, 1955) or infinite frequency (Stoneley, 1949). The former authors consider, without proof, anisotropy to be the limiting case of a laminated solid as the thickness of the layers becomes infinitesimal,

and Stoneley considers surface wave propagation along the surface of a half-space.

Surface wave studies on bounded, layered or inhomogeneous media are more complicated and because of the introduction of dimensions or characteristic lengths demand frequency information that is not available in the study of limiting cases.

We solve exactly the complete boundary value problem for surface wave propagation in layered anisotropic media and, in certain cases, demonstrate the degree of approximation involved in previous studies.

We will first consider materials that possess an axis of symmetry in the sense that all rays at right angles to this axis are equivalent. Such media are called "transversely isotropic" and wave propagation in infinite or semi-infinite media with this symmetry has been discussed by Love (1944), Satô (1950), Musgrave (1959), and Stoneley (1949) with a convenient summary in Mason (1958) and Ewing et al. (1957). Transverse isotropy results in the same set of elastic constants as that for hexagonal symmetry and hence is exhibited in all metals or minerals crystallizing in the hexagonal system. This symmetry can also be expected in sediments, planar igneous bodies, floating ice sheets and rolled or extruded metal and plastic sheets. This latter material is often used in two-dimensional model experiments.

An isotropic solid is governed by two elastic constants and the characteristic equation has three roots, one corresponding to a com-

pressional wave and a double root corresponding to the two polarizations of the distortional wave. These velocities are independent of direction. A transversely isotropic solid is governed by five elastic constants, and the separation into two waves, one for which the curl of the displacement vanishes and one for which the divergence of the displacement vanishes does not in general occur. Corresponding to any assigned wave normal there are three velocities of elastic wave propagation and only in special cases do these degenerate to purely shear and purely compressional motion.

II. GENERALIZED HOOKE'S LAW AND THE EQUATIONS OF MOTION

Ignoring body forces the equations of small motion are three of the form,

$$\rho \frac{\partial^2 u}{\partial t^2} = \frac{\partial p_{xx}}{\partial x} + \frac{\partial p_{xy}}{\partial y} + \frac{\partial p_{xz}}{\partial z} \tag{1}$$

The stresses p_{ij} are derived from the strain energy function W by

$$p_{xx} = \frac{\partial W}{\partial e_{xx}}, \qquad p_{xy} = \frac{\partial W}{\partial e_{xy}}, \quad \text{etc.} \tag{2}$$

where (Love, 1944)

$$2W = c_{11}(e_{xx}^2 + e_{yy}^2) + c_{33}e_{zz}^2 + 2c_{13}(e_{xx} + e_{yy})e_{zz} + 2c_{12}e_{xx}e_{yy} + c_{44}(e_{yz}^2 + e_{zx}^2) + \left(\frac{c_{11} - c_{12}}{2}\right)e_{xy}^2 \tag{3}$$

for media with hexagonal or transverse isotropic symmetry. Five independent elastic constants are required to specify completely the elastic behavior of such material.

The stresses are, accordingly

$$\begin{aligned}
p_{xx} &= c_{11}e_{xx} + c_{12}e_{yy} + c_{13}e_{zz} \\
p_{yy} &= c_{12}e_{xx} + c_{11}e_{yy} + c_{13}e_{zz} \\
p_{zz} &= c_{13}(e_{xx} + e_{yy}) + c_{33}e_{zz} \\
p_{yx} &= p_{xy} = \left(\frac{c_{11} - c_{12}}{2}\right)e_{xy} \\
p_{zy} &= p_{yz} = c_{44}e_{yz} \\
p_{xz} &= p_{zx} = c_{44}e_{xz}
\end{aligned} \tag{2a}$$

From the symmetry of the above equations it is obvious that z has been taken as the unique axis.

The matrix of the elastic constants for media with hexagonal or transverse isotropic symmetry is therefore

$$\begin{matrix} c_{11} & c_{12} & c_{13} & 0 & 0 & 0 \\ c_{12} & c_{11} & c_{13} & 0 & 0 & 0 \\ c_{13} & c_{13} & c_{33} & 0 & 0 & 0 \\ 0 & 0 & 0 & c_{44} & 0 & 0 \\ 0 & 0 & 0 & 0 & c_{44} & 0 \\ 0 & 0 & 0 & 0 & 0 & \frac{c_{11}-c_{12}}{2} \end{matrix}$$

For an isotropic body,

$$c_{11} = c_{33} = \lambda + 2\mu; \quad c_{13} = \lambda; \quad \frac{c_{11}-c_{12}}{2} = c_{44} = \mu$$

The equations of motion become,

$$\rho \frac{\partial^2 u}{\partial t^2} = c_{11}\frac{\partial^2 u}{\partial x^2} + \left(\frac{c_{11}-c_{12}}{2}\right)\frac{\partial^2 u}{\partial y^2} + c_{44}\frac{\partial^2 u}{\partial z^2} + c_{12}\frac{\partial^2 v}{\partial x \partial y} + c_{13}\frac{\partial^2 w}{\partial x \partial z} + \left(\frac{c_{11}-c_{12}}{2}\right)\frac{\partial^2 v}{\partial x \partial y} + c_{44}\frac{\partial^2 w}{\partial x \partial z}$$

$$\rho \frac{\partial^2 v}{\partial t^2} = \left[\frac{c_{11}-c_{12}}{2}\right]\left[\frac{\partial^2 u}{\partial x \partial y} + \frac{\partial^2 v}{\partial x^2}\right] + c_{12}\frac{\partial^2 v}{\partial y^2} + c_{11}\frac{\partial^2 v}{\partial y^2} + c_{12}\frac{\partial^2 w}{\partial z \partial y} + c_{44}\frac{\partial^2 v}{\partial z^2}$$

$$\rho \frac{\partial^2 w}{\partial t^2} = c_{44}\left[\frac{\partial^2 w}{\partial x^2} + \frac{\partial^2 v}{\partial y \partial z} + \frac{\partial^2 w}{\partial y^2} + \frac{\partial^2 u}{\partial x \partial z}\right] + c_{13}\left[\frac{\partial^2 u}{\partial x \partial z} + \frac{\partial^2 v}{\partial y \partial z}\right] + c_{33}\frac{\partial^2 w}{\partial z^2}$$

where u, v, w are the displacements in the x, y, z directions. There is no advantage in introducing potentials since the equations of motion are still not separable.

III. PLANE WAVES IN AN INFINITE MEDIUM

The theory of plane wave propagation in the interior of an infinite anisotropic body is well developed (see for instance Love [1944] or Mason [1958]). We begin with a brief review of this theory to establish the setting for the following sections.

For plane waves propagated in a direction specified by direction cosines (ℓ, m, n) we take

$$(u, v, w) = (U, V, W)e^{i\omega t}e^{-ik(\ell x + my + nz)}$$

Substitution into the equations of motion gives,

$$\begin{bmatrix} \mathcal{F} - \rho c^2 & \ell m\left(\frac{c_{11}+c_{12}}{2}\right) & n\ell(c_{13}+c_{44}) \\ \ell m\left(\frac{c_{11}+c_{12}}{2}\right) & \mathcal{G} - \rho c^2 & mn(c_{13}+c_{44}) \\ n\ell(c_{13}+c_{44}) & mn(c_{13}+c_{44}) & \mathcal{H} - \rho c^2 \end{bmatrix} \begin{bmatrix} U \\ V \\ W \end{bmatrix} = 0 \qquad (5)$$

where

$$\begin{aligned} \mathcal{F} &= \ell^2 c_{11} + m^2\left(\frac{c_{11}-c_{12}}{2}\right) + n^2 c_{44} \\ \mathcal{G} &= \ell^2\left(\frac{c_{11}-c_{12}}{2}\right) + m^2 c_{11} + n^2 c_{44} \\ \mathcal{H} &= (\ell^2 + m^2)c_{44} + n^2 c_{33} \end{aligned} \qquad (6)$$

By setting the determinant of the coefficients equal to zero, we obtain the velocity equation. Two special cases may be dealt with immediately:

a.) For transmission along the unique axis, $n = 1$, $m = \ell = 0$, $c^2 = c_{33}/\rho$ and $c^2 = c_{44}/\rho$ are solutions. The first corresponds to a

vertically travelling purely compressional wave (PV) and the second is a double root corresponding to a vertically travelling shear wave with horizontal particle motion. The degeneracy is caused by the SV and SH waves becoming indistinguishable.

b.) For transmission along the x or y direction or any other direction perpendicular to the z-axis, $n = 0$ the solutions are:

$$c^2 = \frac{c_{11}}{\rho} \qquad \text{compressional, PH}$$

$$c^2 = \frac{c_{44}}{\rho} \qquad \text{shear, SV}$$

$$c^2 = \frac{c_{11} - c_{12}}{2\rho} \qquad \text{shear, SH}$$

Therefore measurement along these two directions will determine 4 of the 5 elastic constants. To determine the fifth we need a measurement at some intermediate angle. In particular we can set $\ell = n = \frac{1}{\sqrt{2}}$, $m = 0$ and from the velocity equation obtain

$$c_{13} = \left[\left(2\rho c^2 - \left[\frac{c_{11} + c_{33} + 2c_{44}}{2}\right]\right)^2 - \left(\frac{c_{11} - c_{33}}{2}\right)^2\right]^{1/2} - c_{44}$$

giving c_{13} in terms of the velocity of the fastest wave travelling at 45° to the z-axis. Solving the velocity equation for arbitrary ℓ, m, n we can determine the directional dependence of the wave velocities.

In the following we will use the designations:

$$\frac{c_{33}}{\rho} = a_2^2 \quad \text{(PV)} \qquad ; \qquad \frac{c_{11}}{\rho} = a_1^2 \quad \text{(PH)}$$

$$\frac{c_{44}}{\rho} = \beta_1^2 \quad (SH_V, SV_V, SV_H) \; ; \quad \frac{c_{11} - c_{12}}{2\rho} = \beta_2^2 \quad (SH_H) \qquad (7)$$

For an isotropic body

$$a_1^2 = a_2^2 = \frac{\lambda + 2\mu}{\rho} \; ; \quad \beta_1^2 = \beta_2^2 = \frac{\mu}{\rho}$$

The wave and velocity surfaces obtained from 5 will not in general be spheres, unlike the isotropic case. The wave surface can be a multi-valued function of direction, depending on the elastic constants, for certain angles of propagation.

IV. SURFACE WAVES IN AN ANISOTROPIC LAYER

Consider now a layer of thickness $2H$ with the above symmetry overlying a fluid halfspace with constants ρ_2, λ_2. Take z increasing downward from the center of the layer. This configuration will permit us to study the effect of anisotropy in a relatively simple system for which the isotropic theory is well developed and for which experimental data are available. Also, with this general case in hand we can easily study as special cases the effect of anisotropy on Rayleigh and Stoneley waves, and on propagation in a free plate. Later we will discuss the general n-layer anisotropic problem and point out how anisotropy will introduce apparent discrepancies between Love and Rayleigh wave data and also give erroneous results for Love or Rayleigh data used alone. Since we will be interested in applying the results of our present restricted problem to a high speed layer overlying a low speed fluid halfspace (the floating ice sheet problem) we have the additional problem of leakage for all modes with phase velocities greater than the fluid velocity but this is resolved by programming our resultant period equation in complex algebra, permitting the location of complex roots. This, however, introduces no additional difficulties in our present analysis.

Restricting ourselves to motion in two dimensions (x, z) we put $\partial/\partial y = 0$, $e_{yy} = 0$, $e_{yz} = 0$, $e_{xy} = 0$.

For surface waves we seek solutions of the type

$$(u, w) = [U(z), W(z)]\, e^{i(\omega t - kx)} \tag{8}$$

Substitution into the equations of motion yields,

$$-\rho_1\omega^2 U(z) = -c_{11}k^2 U(z) - ik(c_{13}+c_{44})W'(z) + c_{44}U''(z)$$
$$-\rho_1\omega^2 W(z) = c_{33}W''(z) - ik(c_{13}+c_{44})U'(z) - k^2 c_{44}W(z) \tag{9}$$

where the primes denote $\partial/\partial z$. These equations are coupled; by differentiating each equation twice the system may be separated, and we obtain the fourth order equations

$$U^{iv}(z) - \left[\frac{\Psi_{11}}{c_{44}} - \frac{k^2G^2}{c_{33}c_{44}} + \frac{\Psi_{44}}{c_{33}}\right] U''(z) + \frac{\Psi_{44}\Psi_{11}}{c_{33}c_{44}} U(z) = 0$$
$$W^{iv}(z) - \left[\frac{\Psi_{44}}{c_{33}} - \frac{k^2G^2}{c_{44}c_{33}} + \frac{\Psi_{11}}{c_{44}}\right] W''(z) + \frac{\Psi_{11}\Psi_{44}}{c_{44}c_{33}} W(z) = 0 \tag{10}$$

where

$$G = c_{13} + c_{44}$$
$$\Psi_{ii} = (c_{ii}k^2 - \rho\omega^2)$$

To find solutions for 10 we first consider the factored equation

$$\left(\frac{\partial^2}{\partial z^2} + \nu_1^2\right)\left(\frac{\partial^2}{\partial z^2} + \nu_2^2\right)\chi = 0 \tag{10a}$$

When expanded this product of one-dimensional Helmholtz operators can be shown to be equivalent to equation 10 with

$$\nu_1^2 + \nu_2^2 = -\frac{\Psi_{11}}{c_{44}} + \frac{k^2G^2}{c_{33}c_{44}} - \frac{\Psi_{44}}{c_{33}}$$
$$\nu_1^2\nu_2^2 = \frac{\Psi_{11}\Psi_{44}}{c_{33}c_{44}} \tag{11}$$

The solution of a factored differential equation such as 10a is equal to the sum of the solutions for each factor. Therefore the solutions are

$$U(z) = \sum_i U_i e^{\nu_i z}, \quad W(z) = \sum_i W_i e^{\nu_i z} \qquad i = 1, 2 \tag{12}$$

where, from 11,

$$(c_{44}\nu^2 - c_{11}k^2 + \rho_1\omega^2)(c_{33}\nu^2 - k^2 c_{44} + \rho_1\omega^2) + k^2\nu^2 G^2 = 0 \tag{13}$$

The explicit values of ν^2 from this are,

$$\nu_i^2 = -\frac{M_1}{2c_{33}c_{44}} \pm \frac{M_3}{2c_{33}c_{44}} \tag{14}$$

where

$$M_3 = [M_1^2 - 4M_2 c_{33}c_{44}]^{1/2}$$

$$M_1 = c_{33}(\rho_1\omega^2 - c_{11}k^2) + c_{44}(\rho_1\omega^2 - c_{44}k^2) + k^2G^2$$

$$M_2 = (\rho_1\omega^2 - c_{11}k^2)(\rho_1\omega^2 - c_{44}k^2)$$

Note that ν_i can become complex for real ω and k, a possibility that does not exist for isotropic media. This means that waves that die off exponentially from the interface do not exist for all possible values of the elastic constants. This phenomenon will be discussed in Chapter IX.

For an isotropic body equation 14 becomes

$$\nu_1^2 = (k^2 - \omega^2/a^2), \quad \nu_2^2 = (k^2 - \omega^2/\beta^2), \quad a^2 = (\lambda+2\mu)/\rho, \quad \beta^2 = \mu/\rho$$

so that ν_1 reduces to the form associated with a pure compressional wave and ν_2 reduces to that for a pure distortional wave.

For a given ν_i the displacement ratios in the solid are,

$$\left(\frac{U}{W}\right)_i = -\frac{k\nu_i G}{(c_{44}\nu_i^2 - c_{11}k^2 + \rho_1\omega^2)} = \frac{(c_{33}\nu_i^2 - k^2 c_{44} + \rho_1\omega^2)}{k\nu_i G} = \frac{1}{\gamma_i} \tag{15}$$

$$W_i = \gamma_i U_i$$

For isotropic media $\gamma_1 = \nu_1/k$, $\gamma_2 = k/\nu_2$. We therefore take as our solutions:

$$U = U_1 \mathrm{sh}\,\nu_1 z + U_2 \mathrm{ch}\,\nu_1 z + U_3 \mathrm{sh}\,\nu_2 z + U_4 \mathrm{ch}\,\nu_2 z \tag{16a}$$

$$W = i\gamma_1 U_1 \mathrm{ch}\,\nu_1 z + i\gamma_1 U_2 \mathrm{sh}\,\nu_1 z + i\gamma_2 U_3 \mathrm{ch}\,\nu_2 z + i\gamma_2 U_4 \mathrm{sh}\,\nu_2 z$$

in the solid, and

$$U^* = U_o e^{-\nu' z}$$
$$W^* = -\frac{i\nu'}{k} U_o e^{-\nu' z} \tag{16b}$$

in the liquid, where

$$\nu'^2 = \left(k^2 - \frac{\omega^2}{a^{*2}}\right); \quad a^{*2} = \frac{\lambda_2}{\rho_2}$$

The boundary conditions are

$$p_{zz} = c_{33}\frac{\partial W}{\partial z} + c_{13}\frac{\partial U}{\partial x} = 0 \qquad p_{zx} = c_{44}\left(\frac{\partial U}{\partial z} + \frac{\partial W}{\partial x}\right) = 0, \; z = -H \tag{17}$$

$$p_{zx} = 0 \qquad p_{zz} = p_{zz}^* \qquad W = W^*, \quad z = H$$

Substituting equations 16 into equations 17 gives,

$$U_1[-\gamma_1\nu_1 c_{33} + c_{13}k]\,\mathrm{sh}\,\nu_1 H + U_2[\gamma_1\nu_1 c_{33} - c_{13}k]\,\mathrm{ch}\,\nu_1 H$$

$$+ U_3[-\nu_2\gamma_2 c_{33} + c_{13}k]\,\mathrm{sh}\,\nu_2 H + U_4[\nu_2\gamma_2 c_{33} - c_{13}k]\,\mathrm{ch}\,\nu_2 H = 0$$

$$U_1[\nu_1 + k\gamma_1]\,\mathrm{ch}\,\nu_1 H + U_2[-\nu_1 - k\gamma_1]\,\mathrm{sh}\,\nu_1 H + U_3[\nu_2 + \gamma_2 k]\,\mathrm{ch}\,\nu_2 H$$

$$+ U_4[-\nu_2 - \gamma_2 k]\,\mathrm{sh}\,\nu_2 H = 0$$

$$U_1[\gamma_1\nu_1 c_{33} - c_{13}k]\,\mathrm{sh}\,\nu_1 H + U_2[c_{33}\gamma_1\nu_1 - c_{13}k]\,\mathrm{ch}\,\nu_1 H$$

$$+ U_3[\nu_2 c_{33}\gamma_2 - c_{13}k]\,\mathrm{sh}\,\nu_2 H + U_4[c_{33}\nu_2\gamma_2 - c_{13}k]\,\mathrm{ch}\,\nu_2 H$$

$$+ U_o \frac{\lambda_2}{k}[k^2 - \nu'^2]\,e^{-\nu' H} = 0 \qquad (18)$$

$$U_1[\gamma_1 k]\,\mathrm{ch}\,\nu_1 H + U_2 k\gamma_1 \mathrm{sh}\,\nu_1 H + U_3 k\gamma_2 \mathrm{ch}\,\nu_2 H + U_4 k\gamma_2 \mathrm{sh}\,\nu_2 H$$

$$+ U_o \nu' e^{-\nu' H} = 0$$

$$U_1[\nu_1 + k\gamma_1]\,\mathrm{ch}\,\nu_1 H + U_2[\nu_1 + k\gamma_1]\,\mathrm{sh}\,\nu_1 H + U_3[\nu_2 + k\gamma_2]\,\mathrm{ch}\,\nu_2 H$$

$$+ U_4[\nu_2 + k\gamma_2]\,\mathrm{sh}\,\nu_2 H = 0$$

The condition that the determinant of the coefficients vanish is,

$$\Pi_1\Omega_2\,\mathrm{sh}\,\nu_1(\Pi_1\Gamma_2\,\mathrm{sh}\,\nu_2\,\mathrm{ch}\,\nu_1 - \Pi_2\Gamma_1\,\mathrm{ch}\,\nu_2\,\mathrm{sh}\,\nu_1)$$

$$+ \Lambda_2\Pi_2\,\mathrm{sh}\,\nu_2(\Pi_2\Gamma_1\,\mathrm{sh}\,\nu_1\,\mathrm{ch}\,\nu_2 - \Pi_1\Gamma_2\,\mathrm{sh}\,\nu_2\,\mathrm{ch}\,\nu_1)$$

$$+ \Pi_1\Omega_1\,\mathrm{ch}\,\nu_1(\Pi_1\Gamma_2\,\mathrm{ch}\,\nu_2\,\mathrm{sh}\,\nu_1 - \Pi_2\Gamma_1\,\mathrm{sh}\,\nu_2\,\mathrm{ch}\,\nu_1)$$

$$+ \Lambda_1\Pi_2\,\mathrm{ch}\,\nu_2(\Pi_2\Gamma_1\,\mathrm{sh}\,\nu_2\,\mathrm{ch}\,\nu_1 - \Pi_1\Gamma_2\,\mathrm{sh}\,\nu_1\,\mathrm{ch}\,\nu_2) = 0 \qquad (19)$$

where

$$\Gamma_1 = [-\gamma_1\nu_1 c_{33} + c_{13}k] \qquad \Pi_1 = [\nu_1 + k\gamma_1]$$

$$\Gamma_2 = [-\nu_2\gamma_2 c_{33} + c_{13}k] \qquad \Pi_2 = [\nu_2 + k\gamma_2]$$

$$\Lambda_1 = \nu'\Gamma_1 \operatorname{sh}\nu_1 + \lambda_2\gamma_1(k^2 - \nu_1'^2)\operatorname{ch}\nu_1$$

$$\Lambda_2 = \nu'\Gamma_1 \operatorname{ch}\nu_1 + \lambda_2\gamma_1(k^2 - \nu'^2)\operatorname{sh}\nu_1 \qquad (20)$$

$$\Omega_1 = \nu_1\Gamma_2 \operatorname{sh}\nu_2 + \lambda_2\gamma_2(k^2 - \nu_1'^2)\operatorname{ch}\nu_2$$

$$\Omega_2 = \nu'\Gamma_2 \operatorname{ch}\nu_2 + \lambda_2\gamma_2(k^2 - \nu_1'^2)\operatorname{sh}\nu_2$$

In this equation we have taken the thickness of the plate as unity. This introduces no loss of generality since the thickness is the only dimension in the problem. For an isotropic layer this yields the period equation given by Press and Ewing (1951).

The asymptotic form of equation 19 for short wavelengths is:

$$(\Pi_1\Gamma_2 - \Pi_2\Gamma_1)[\nu'(\Pi_1\Gamma_2 - \Pi_2\Gamma_1) + \lambda_2(k^2 - \nu_1'^2)(\Pi_1\gamma_2 - \Pi_2\gamma_1)] = 0 \qquad (19a)$$

It will later be shown that the first factor is the Rayleigh factor for an anisotropic medium and the second factor is the Stoneley factor for the interface between an anisotropic solid and a fluid.

V. FREE PLATE

By setting $\rho_2 = 0$ the period equation factors into:

$$\left[\frac{\tanh \nu_1 H}{\tanh \nu_2 H}\right]^{\pm 1} = \frac{[\nu_1 + k\gamma_1][\nu_2\gamma_2 c_{33} - c_{13}k]}{[\gamma_1\nu_1 c_{33} - c_{13}k][\nu_2 + \gamma_2 k]} = \frac{\Gamma_2 \Pi_1}{\Gamma_1 \Pi_2} \tag{21}$$

the upper sign corresponding to antisymmetrical waves and the lower sign corresponding to symmetrical waves in a free plate.

In the long wave length limit this becomes:

$$\left[\frac{\nu_1}{\nu_2}\right]^{\pm 1} = \frac{\Gamma_2 \Pi_1}{\Gamma_1 \Pi_2} \tag{22}$$

For symmetrical waves this gives

$$c_{33}(\rho\omega^2/k^2) - (c_{11}c_{33} - c_{13}^2) = 0 \tag{22a}$$

We can also derive the long wave length limit for symmetrical waves from plane stress theory. Taking as before the xy plane parallel to the surface of the plane and propagation in the x-direction we have

$$\frac{\partial p_{xx}}{\partial x} = \rho \frac{\partial^2 u}{\partial t^2}$$

Eliminating $\partial w/\partial z$ from the first and third of equations 3,

$$p_{xx} = \frac{(c_{11}c_{33} - c_{13}^2)}{c_{33}} \frac{\partial u}{\partial x} \tag{23a}$$

Therefore

$$\rho \frac{\partial^2 u}{\partial t^2} = \left(\frac{c_{11}c_{33} - c_{13}^2}{c_{33}}\right) \frac{\partial^2 u}{\partial x^2} \tag{23b}$$

and the plate velocity c_p is:

$$c_p^2 = \frac{c_{11}c_{33} - c_{13}^2}{\rho c_{33}} \tag{24}$$

in agreement with 22a.

This will serve as a check on the low frequency limit of our ensuing calculations. Note that the plate velocity does not depend only on the horizontal compressional and SV velocities as we may have suspected for the long wave limit but involves the constants in the vertical and intermediate directions as well. In particular this can lead to plate velocities which are outside the range possible for an isotropic solid and this holds true also for the rest of the dispersion curve. This is related to the fact that directional Poisson's ratios in an anisotropic solid can exceed 0.5.

For waves short compared to the layer thickness the hyperbolic tangents can be replaced by unity giving

$$\Gamma_2 \Pi_1 - \Gamma_1 \Pi_2 = 0 \tag{25}$$

for both symmetrical and antisymmetrical motion.

This is, again, the Rayleigh equation for anisotropic media.

VI. RAYLEIGH AND STONELEY WAVES

Consider an anisotropic halfspace with the above properties. Assume solutions that decrease exponentially with depth (z is positive downward and the solid lies in the top half space):

$$\begin{aligned} U &= U_1 e^{\nu_1 z} + U_3 e^{\nu_2 z} \\ W &= i\gamma_1 e^{\nu_1 z} U_1 + i\gamma_2 e^{\nu_2 z} U_3 \end{aligned} \tag{26}$$

The ν_i and γ_i are the same as derived previously for the general case. Applying the condition of a traction free surface we obtain the period equation:

$$R = -\Gamma_1 \Pi_2 + \Gamma_2 \Pi_1 = 0 \tag{27}$$

This is the Rayleigh equation for transversely isotropic media and was first derived by Stoneley [1949]. It reduces in the case of isotropy to:

$$R = [\nu_2^2 + k^2]^2 - 4\nu_1 \nu_2 k^2 = 0 \tag{28}$$

For Stoneley waves we assume motion dying off into both the fluid and the solid. Assume equation 26 for motion in the solid, and, for the fluid:

$$\begin{aligned} U^* &= U_o e^{-\nu' z} \\ W^* &= -\frac{i\nu'}{k} U_o e^{-\nu' z} \end{aligned} \tag{4b}$$

Applying the conditions of a stress free interface and continuity of vertical displacement we obtain the Stoneley period equation:

$$\frac{\lambda_2(k^2 - \nu'^2)}{\nu'} = \frac{\Pi_1\Gamma_2 - \Pi_2\Gamma_1}{\gamma_1\Pi_2 - \gamma_2\Pi_1} \tag{29}$$

For isotropy this goes into

$$R + \delta = 0 \tag{30}$$

where

$$\delta = \frac{\rho_2 a^{*2} \nu_1}{\rho_1 \beta_1^2 \nu'} (\nu_2^2 - k)(\nu'^2 - k^2) \tag{31}$$

This is the form of the Stoneley equation given by Press and Ewing (1951). When $\rho_2 = 0$ we obtain the Rayleigh equation in both the isotropic and anisotropic case. Thus, as we indicated earlier the high frequency limit of the fundamental symmetric and antisymmetric modes of a free plate is the Rayleigh velocity. A floating plate has two branches of the fundamental mode, one corresponding to the Rayleigh velocity and the other to the Stoneley velocity.

VII. LOVE WAVES

In layered transversely isotropic media Love waves exist independently of Rayleigh waves, that is, there is no coupling between Rayleigh type and Love type motion for waves propagating in a plane perpendicular to the unique axis. This is the lowest symmetry for which this coupling does not, in general, exist.

Considering a free layer and taking the axes as before the equations of motion can be satisfied by putting $u = w = 0$, $\frac{\partial}{\partial y} = 0$. For waves of the Love type we take

$$v = V(z)e^{i(\omega t - kx)} = (v_1 \mathrm{sh}\,\zeta z + v_2 \mathrm{ch}\,\zeta z)e^{i(\omega t - kx)} \tag{32}$$

and obtain the reduced wave equation

$$\frac{\partial^2 v}{\partial t^2} = \frac{k^2}{L}(N - \zeta c^2)v \tag{33}$$

so that

$$\zeta^2 = \frac{k^2}{L}(N - \rho c^2) \tag{34}$$

where $N = (c_{11} - c_{12})/2$, $L = c_{44}$. When $L = N = \mu = \rho\beta^2$ we have isotropy and

$$\zeta^2 = (k^2 - \frac{\omega^2}{\beta^2})$$

The boundary conditions are

$$\sigma_{zy} = L\frac{\partial v}{\partial z} = 0 \quad \text{at} \quad z = \pm H$$

These conditions lead to the period equation,

$$\tanh 2kH\left(\frac{N - \rho c^2}{L}\right)^{1/2} = 0 \tag{35}$$

If $\rho c^2 < N$ no roots of the above equation exist. Therefore we must have $\rho c^2 \geq N$, or $c^2 \geq \beta_2^2$. The period equation can therefore be written

$$\tan 2kH(N/L)^{1/2}[(c^2/\beta_2^2) - 1]^{1/2} = 0 \qquad (36)$$

Equation 36 is satisfied if

$$2kH(N/L)^{1/2}[(c^2/\beta_2^2) - 1]^{1/2} = n\pi \quad \text{where} \quad n = 0, 1, 2, \ldots \qquad (37)$$

which is the Love period equation for a free anisotropic plate.

This differs by a factor of $(N/L)^{1/2}$ from the isotropic Love wave period equation. The above derivation also holds for an anisotropic layer in contact with a fluid layer on one or both sides.

As Stoneley (1949) has pointed out, it is the modulus c_{44} that resembles the isotropic rigidity for Rayleigh wave motion, whereas the corresponding modulus for Love wave motion is $(c_{11} - c_{12})/2$. This holds true for layered anisotropic media in general and will make the velocity structure as determined for Rayleigh wave data inconsistent with Love wave information unless the anisotropy is taken into account.

For an anisotropic layer of thickness $2H$ with constants L_1, N_1, and β_2 over an anisotropic halfspace with constants L_2, N_2, and β^* we obtain for Love waves

$$\tan 2kH\left(\frac{c^2}{\beta_2^2} - 1\right)^{1/2}\left(\frac{N_1}{L_1}\right)^{1/2} = \left(\frac{L_2N_2}{L_1N_1}\right)^{1/2}\left(\frac{1 - (c^2/\beta^{*2})}{c^2/\beta_2^2 - 1}\right)^{1/2}$$

In the corresponding isotropic case $N = L = \mu$ and we recover the Love equation in familiar form. Stoneley's (1949) derivation of the anisotropic Love equation is in error.

The general case of Love wave propagation in multi-layered media will be considered in Chapter IX.

It can be shown that the period equation expresses the condition of constructive interference between multi-reflected plane SH waves. This condition may be written, for the free plate

$$4H \cos \theta = n\ell_o \tag{38}$$

where θ is the angle the ray makes with the vertical and ℓ_o is the wavelength measured along the ray. The velocity of SH waves satisfies the equation

$$\rho\beta^2(\theta) = \ell^2 N + n^2 L \tag{39}$$

With the substitutions $\beta(\theta)/c = \sin \theta$, $k = 2\pi \sin \theta/\ell_o$, $\beta_1^2 = L/\rho$ and $\beta_2^2 = N/\rho$ we can write for equations 38 and 39

$$n\pi = \frac{2kHc}{\beta(\theta)} \left[1 - (\beta^2(\theta)/c^2)\right]^{1/2} \tag{38a}$$

$$\beta^2(\theta) = \frac{L}{N} c^2 \left(\frac{c^2}{\beta_2^2} - 1 + \frac{L}{N} \right)^{-1} \tag{39a}$$

Substitution of equation 39a into equation 38a gives the period equation,

$$2kH(N/L)^{1/2} \left[(c^2/\beta_2^2) - 1 \right]^{1/2} = n\pi \tag{40}$$

in agreement with 37.

VIII. NUMERICAL RESULTS

The general period equation 19 was programmed for the Cal Tech Computing Center's Burroughs 220 electronic digital computer, using a complex root finding technique sub-routine developed by Phinney (1961). Modifications were built into the program making it possible to solve for the symmetrical and antisymmetrical modes in a free plate and to evaluate the Rayleigh and Stoneley equations.

We have calculated the dispersion of Rayleigh type waves in plates for three solids which exhibit hexagonal symmetry: a) beryl, b) ice, and c) a laminated solid. These results, of course, apply also to any anisotropic solid having the same relationship between the elastic constants as one of the above examples.

Beryl was chosen in order to extend Stoneley's results to a free plate. Ice was chosen as an example of a solid which exhibits a rather strong anisotropy and because lake ice commonly forms with a vertical c-axis (the unique axis) orientation. The other axes are randomly oriented but since the single crystal has elastic rotational symmetry about the c-axis the result is a large plate having the properties of a single crystal. Sea ice and some lake ice form with a c-axis horizontal orientation. Here again we have a large plate with transverse isotropy but the effective elastic constants are not the same as for a single crystal. A laminated solid is transversely isotropic about the normal to the laminations for long wave lengths; the effective elastic constants must obey certain ordering rules which restricts the extent to which anisotropy may be approximated by layering. Table 1 gives the elastic constants used in computing these three cases.

TABLE 1

Material	c_{11}/c_{44}	c_{33}/c_{44}	c_{12}/c_{44}	c_{13}/c_{44}	φ	ξ	η	ρ (g/cc)
Beryl	4.13	3.62	1.47	1.01	0.88	1.33	0.47	2.7
Ice	4.70	4.96	2.27	1.60	1.05	1.21	1.69	0.917
Layered	4.54	3.32	1.64	1.31	0.73	1.45	2.06	2.4

To show more clearly the effect of anisotropy we have also calculated the dispersion for equivalent isotropic ice, that is $\alpha = \alpha_1$, $\beta = \beta_1$, and for some intermediate cases.

For convenience we introduce the following "anisotropy factors"

$$\varphi = \frac{c_{33}}{c_{11}} \qquad \text{i. e.} \quad a_2^2 = \varphi a_1^2$$

$$\xi = \frac{c_{11} - c_{12}}{2c_{44}} \qquad \beta_1^2 = \xi \beta_2^2 \tag{41}$$

$$\eta = \frac{c_{11} - 2c_{44}}{c_{13}}$$

Isotropic media have $\varphi = \xi = \eta = 1$.

Figure 1 shows the effect on M_{11} of increasing all of the anisotropy factors from below 1 to the values attained by anisotropic ice. For this kind of anisotropy, i. e. φ, ξ and η increasing, the dispersion curve migrates uniformly toward higher phase velocity. The low frequency limit of M_{11} for an isotropic plate satisfies

$$\frac{c^2}{\beta^2} = 4\left(1 - \frac{\beta^2}{a^2}\right)$$

Therefore $(c_p/\beta) \leq 2$. For an anisotropic plate with the constants of ice equation 24 gives $(c_p/\beta_1) = 2.045$. This agrees with the numerical evaluation of the general period equation.

Stoneley (1949) has previously noted that the Rayleigh velocity for an anisotropic solid can be higher than that for a Poisson solid;

we note, in addition, that it can be higher than is theoretically possible for an isotropic solid. This is true in particular for solids with the constants of beryl and ice. Therefore both ends of M_{11} are greater than the theoretical maximum under the assumption of isotropy.

To pursue this point further we plotted in fig. 2 the variation of the four lowest modes of an isotropic plate as Poisson's Ratio changed from 0.25 to 0.5, the latter case indicating incompressibility. The data is from Satô (1951). It is of interest to note that Poisson's Ratio has a much greater effect on the symmetrical modes than on the antisymmetrical ones. This is to be expected since we have effectively held β constant while changing α, and the M_1 modes are chiefly compressional in nature while the M_2 modes tend to couple with an ideal free shear mode (Tolstoy, 1957). Plotted for comparison are the four lowest modes for ice and M_{11} for beryl. All the modes except M_{21} (the flexural mode) which is not drawn, and the low frequency end of M_{11} for beryl, are well outside the theoretical limit of isotropic plates. M_{21} for ice deviates slightly from the theoretical range at both ends.

In fig. 3 are the complete results for ice, for M_{11} thru M_{22}. Note the negative group velocity tail on M_{12}. This phenomenon has been discussed by Tolstoy (1957), who attributes it to a negative phase velocity rather than an actual backward propagation of energy.

Figure 4 gives the results for a laminated plate consisting of alternating layers of sandstone and limestone in the ratio 3 to 1. The effective elastic constants for infinite wave length in this medium have

been computed by Postma (1955) and are listed in table 1. The anisotropy factors are $\varphi = 0.733$, $\xi = 1.450$ and $\eta = 2.0576$, making the anisotropy of this material quite different from beryl or ice. Note the pulling down of the group velocity minimum, and in particular, the accentuated negative group velocity "tail."

The Stoneley wave equation was evaluated numerically for $\rho_2/\rho_1 = 1.12$ (the water to ice density ratio) and several a^*/β_1 ratios. As in the isotropic case the Stoneley velocity is always a fraction of the slower of a^*, β_1 but, for the constants tested, is a larger fraction than for the corresponding isotropic case. For example when a^*/β_1 takes on the values 0.79, 0.9, 1.0, 1.1 and 1.2 the Stoneley velocity c_{ST}/β_1 is 0.70, 0.74, 0.76, 0.78, and 0.79 for the anisotropic case and 0.67, 0.71, 0.72, 0.74 and 0.75 for the isotropic case.

IX. MATRIX FORMULATION OF THE GENERAL LAYERED PROBLEM

Rayleigh Waves

Following Haskell (1953) we now show how the solution of the wave propagation problem in a single anisotropic layer leads naturally to the n-layer problem. The normalized velocities and stresses in the mth layer can be written, (understanding an $e^{i(\omega t-kx)}$ factor)

$$\frac{\dot{u}}{c} = [\, ik\,sh\nu_{1_m}\, zU_{1_m} + ki\,ch\nu_{1_m}\, zU_{2_m} + ik\,sh\nu_{2_m}\, U_{3_m} + ik\,ch\nu_{2_m}\, zU_{4_m}\,]$$

$$\frac{\dot{w}}{c} = [\, -k\gamma_{1_m}\, ch\nu_{1_m}\, zU_{1_m} - k\gamma_{1_m}\, sh\nu_{1_m}\, zU_{2_m} - k\gamma_{2_m}\, ch\nu_{2_m}\, zU_{3_m}$$

$$- k\gamma_{2_m}\, sh\nu_{2_m}\, zU_{4_m}\,] \tag{42}$$

$$p_{zz} = i(\gamma_{1_m}\nu_{1_m} C_m - F_m k)sh\nu_{1_m}\, zU_{1_m} + i(C_m\gamma_{1_m}\nu_{1_m} - F_m k)ch\nu_{1_m}\, zU_{2_m}$$

$$+ i(\gamma_{2_m}\nu_{2_m} C_m - F_m k)sh\nu_{2_m}\, zU_{3_m} + i(\gamma_{2_m}\nu_{2_m} C_m - F_m k)ch\nu_{2_m}\, zU_{4_m}$$

$$p_{xz} = L(\nu_{1_m} + k\gamma_{1_m})ch\nu_{1_m}\, zU_{1_m} + L_m(\nu_{1_m} + k\gamma_{1_m})sh\nu_{1_m}\, zU_{2_m}$$

$$+ L_m\nu_{2_m} + \gamma_{2_m} k)ch\nu_{2_m}\, zU_{3_m} + L_m(\nu_{2_m} + \gamma_{2_m} k)sh\nu_{2_m}\, zU_{4_m}$$

where C, L and F are the elastic constants c_{33}, c_{44} and c_{13}. The boundary conditions to be met at each solid-solid interface are that these four quantities be continuous. The geometry under consideration and the numbering of the layers and interfaces is shown in figure 5.

Taking $z = 0$ at the $(m-1)^{th}$ interface the linear relationship between the motion stress vector and the displacement coefficients can be written

$$(\dot{u}_{m-1}/c,\ \dot{w}_{m-1}/c,\ p_{zz_{m-1}},\ p_{xz_{m-1}}) = E_m(U_m, V_m, W_m, Z_m) \tag{43}$$

where

$$(U_1, U_2, U_3, U_4)_m = (U_m, V_m, W_m, Z_m)$$

and where E_m is the matrix

$$E_m = \begin{bmatrix} 0 & ik & 0 & ik \\ -k\gamma_{1_m} & 0 & -k\gamma_{2_m} & 0 \\ 0 & i(C_m\gamma_{1_m}\nu_{1_m} - F_m k) & 0 & i(C_m\nu_{2_m}\gamma_{2_m} - F_m k) \\ L_m(\nu_{1_m} + k\gamma_{1_m}) & 0 & L_m(\nu_{2_m} + k\gamma_{2_m}) & 0 \end{bmatrix} \tag{44}$$

Setting $z = d_m$ we can write the relationship between the motion stress vector of the mth interface and the U_{i_m},

$$(\dot{u}_m/c, \dot{w}_m/c, p_{zz_m}, p_{xz_m}) = D_m(U_m, V_m, W_m, Z_m) \tag{45}$$

where D_m is the matrix

$$
D_m = \begin{vmatrix}
ik\,sh\,\nu_{1_m} d_m & ik\,ch\,\nu_{1_m} d_m & ik\,sh\,\nu_{2_m} d_m & ik\,ch\,\nu_{2_m} d_m \\
-k\gamma_{1_m} ch\,\nu_{1_m} d_m & -k\gamma_{1_m} sh\,\nu_{1_m} d_m & -k\gamma_{2_m} ch\,\nu_{2_m} d_m & -k\gamma_{2_m} sh\,\nu_{2_m} d_m \\
\left\{i(\gamma_{1_m}\nu_{1_m} C_m - F_m k) sh\,\nu_{1_m} d_m\right\} & \left\{i(C_m\gamma_{1_m}\nu_{1_m} - F_m k) ch\,\nu_{1_m} d_m\right\} & \left\{i(\nu_{2_m}\gamma_{2_m} C_m - F_m k) sh\,\nu_{2_m} d_m\right\} & \left\{i(C_m\nu_{2_m}\gamma_{2_m} - F_m k) ch\,\nu_{2_m} d_m\right\} \\
L_m(\nu_{1_m} + k\gamma_{1_m}) ch\,\nu_{1_m} d_m & L_m(\nu_{1_m} + k\gamma_{1_m}) sh\,\nu_{1_m} d_m & L_m(\nu_{2_m} + \gamma_{2_m} k) ch\,\nu_{2_m} d_m & L_m(\nu_{2_m} + \gamma_{2_m} k) sh\,\nu_{2_m} d_m
\end{vmatrix} \tag{46}
$$

The coefficients U_i may be eliminated between equations 43 and 46 giving a linear relationship between the motion stress vector at the bottom and the top of the mth layer,

$$(\dot{u}_m/c, \dot{w}_m/c, p_{zz_m}, p_{xz_m})$$

$$= D_m E_m^{-1} (\dot{u}_{m-1}/c, \dot{w}_{m-1}/c, \sigma_{zz_{m-1}}, \sigma_{xz_{m-1}}) \qquad (47)$$

The inverse of E_m is given by

$$ikE_m^{-1} = \begin{bmatrix} 0 & \dfrac{i(\nu_{2_m} + k\nu_{2_m})}{(\gamma_{1_m}\nu_{2_m} - \gamma_{2_m}\nu_{1_m})} & 0 & \dfrac{-i\gamma_{2_m} k}{L_m(\gamma_{1_m}\nu_{2_m} - \gamma_{2_m}\nu_{1_m})} \\ \dfrac{-(C_m\gamma_{2_m}\nu_{2_m} - kF_m)}{C_m(\gamma_{1_m}\nu_{1_m} - \gamma_{2_m}\nu_{2_m})} & 0 & \dfrac{k}{C_m(\gamma_{1_m}\nu_{1_m} - \gamma_{2_m}\nu_{2_m})} & 0 \\ 0 & \dfrac{i(\nu_{1_m} + k\gamma_{1_m})}{(\gamma_{1_m}\nu_{2_m} - \gamma_{2_m}\nu_{1_m})} & 0 & \dfrac{i\gamma_{1_m} k}{L_m(\gamma_{1_m}\nu_{2_m} - \gamma_{2_m}\nu_{1_m})} \\ \dfrac{(C_m\gamma_{1_m}\nu_{1_m} - kF_m)}{C_m(\gamma_{1_m}\nu_{1_m} - \gamma_{2_m}\nu_{2_m})} & 0 & \dfrac{-k}{C_m(\gamma_{1_m}\nu_{1_m} - \gamma_{2_m}\nu_{2_m})} & 0 \end{bmatrix} \tag{48}$$

Applying equation 47 recursively we may carry our solution down through a stack of n-layers, just as in the isotropic case.

See Harkrider and Anderson (1962) for details concerning the programming of equation 47.

The most serious problem in computing dispersion on multi-layered media is the possibility of ν_i becoming complex. When this occurs the displacement does not die off as a pure exponential into the half-space and Rayleigh waves, in the classic sense, do not exist.

The condition that ν_i^2 be real is

$$M_1^2 - 4M_2 c_{33} c_{44} > 0$$

This relation has been evaluated for four different Poisson type relations between the elastic constants. The area below the appropriate curve in figure 6 is forbidden to Rayleigh waves. Note that only isotropic media, i.e. $\varphi = 1$, can always support Rayleigh waves. Even a slight departure from isotropy can put us in a forbidden region for sufficiently small phase velocity. This illustrates in a striking fashion the unique position of isotropy in the theory of elastic wave propagation.

Love Waves

The extension of the Love wave theory to multi-layered media is somewhat simpler and will be developed in detail.

Consider plane waves of angular frequency ω propagated in the positive x-direction with phase velocity c in a semi-infinite medium composed of n parallel homogeneous transversely isotropic layers. The n^{th} layer is an anisotropic half-space. The geometry

under consideration and the numbering of the layers and interfaces is the same as in figure 5. The following technique is similar to that developed by Haskell (1951) for isotropic layers.

Associated with the m^{th} layer are its density, ρ_m, thickness, d_m, and directional rigidities, N_m and L_m. The equation of Love type motion in the m^{th} layer is

$$\rho_m \frac{\partial^2 v_m}{\partial t^2} = N_m \frac{\partial}{\partial x} e_{xy} + L_m \frac{\partial}{\partial z} e_{yz} \tag{49}$$

where

$$N_m = \left(\frac{c_{11} - c_{12}}{2} \right)_m = (\rho\beta_2^2)_m$$

$$L_m = (c_{44})_m = (\rho\beta_1^2)_m$$

β_1 = vertical SH velocity

β_2 = horizontal SH velocity

v = horizontal transverse displacement

The velocity of SH waves satisfies the equation (Stoneley, 1949)

$$\rho\beta^2 = \ell^2 N + n^2 L \tag{50}$$

where ℓ and n are the direction cosines from the x and z axes. For isotropic media $L = N = \mu$ and $\rho\beta^2 = \mu$ since $\ell^2 + n^2 = 1$.

Figure 7 shows schematically the velocity surface of a wave satisfying this equation.

The strains are

$$e_{xy} = \frac{\partial v}{\partial x} \quad \text{and} \quad e_{yz} = \frac{\partial v}{\partial z} \tag{51}$$

from which we obtain

$$\rho_m \frac{\partial^2 v_m}{\partial t^2} = N_m \frac{\partial^2 v_m}{\partial x^2} + L_m \frac{\partial^2 v_m}{\partial z^2} \tag{52}$$

This is the displacement equation of motion for SH type motion in transversely isotropic material satisfied in each layer.

The plane wave solution of equation 52 for an anisotropic layer is

$$u = w = 0$$

$$v = [\, V_1 e^{-ik\zeta z} + V_2 e^{ik\zeta z}\,] e^{i(\omega t - kx)} \tag{53}$$

where V_1 and V_2 are constants.

Substitution into the equation of motion yields,

$$\rho\omega^2 = Nk^2 + Lk^2\zeta^2 \tag{54}$$

or

$$\zeta = \left(\frac{N}{L}\right)^{1/2} \left(\frac{c^2}{\beta_2^2} - 1\right)^{1/2}$$

The boundary conditions to be satisfied are that the transverse component of displacement, v, and the transverse shear stress, p_{yz}, be continuous at each interface.

The transverse shear stress is

$$p_{yz} = L \frac{\partial v}{\partial z} = ik\zeta L[\, -V_i e^{-ik\zeta z} + V_2 e^{ik\zeta z}\,] e^{i(\omega t - kx)} \tag{55}$$

Following Haskell we will relate the displacement-stress vectors at the bottom and top of each layer. This relation plus the interface and

infinity conditions are sufficient to determine motion at depth in terms of the surface conditions.

Taking the origin of z at the $(m-1)^{th}$ interface we have, at this interface

$$\begin{aligned}(\dot{v}/c)_{m-1} &= ik(V_1 + V_2)_m \\ (p_{zy})_{m-1} &= ikL_m\zeta_m(-V_1+V_2)_m\end{aligned} \tag{56}$$

where $c = \omega/k$ is the phase velocity and is the same for all layers.

At the m^{th} interface

$$\begin{aligned}(\dot{v}/c)_m &= ik(V_1 e^{ik\zeta_m d_m} + V_2 e^{ik\zeta_m d_m}) \\ (p_{zy})_m &= iL_m k\zeta_m(-V_1 e^{-ik\zeta_m d_m} + V_2 e^{ik\zeta_m d_m})\end{aligned} \tag{57}$$

By eliminating V_1 and V_2 between equations 56 and 57 we obtain

$$\begin{aligned}(\dot{v}/c)_m &= (\dot{v}/c)_{m-1}\cos k\zeta_m d_m + \frac{i}{L_m\zeta_m}(p_{zy})_{m-1}\sin k\zeta_m d_m \\ (p_{zy})_m &= iL_m\zeta_m(\dot{v}/c)_{m-1}\sin k\zeta_m d_m + (p_{zy})_{m-1}\cos k\zeta_m d_m\end{aligned} \tag{58}$$

This is a relation between the stress-displacement vectors at the top and bottom of the m^{th} layer and can be written

$$(\dot{v}/c, p_{zy})_m = a_m(\dot{v}/c, p_{zy})_{m-1} \tag{59}$$

where a_m is the matrix

$$a_m = \cos k\zeta_m d_m \begin{bmatrix} 1 & \frac{i}{L_m \zeta_m} \tan k\zeta_m d_m \\ iL_m \zeta_m \tan k\zeta_m d_m & 1 \end{bmatrix} \tag{60}$$

By repeated application we have

$$\begin{aligned} (\dot{v}/c, p_{zy})_{n-1} &= a_{n-1} a_{n-2} \cdots a_1 (\dot{v}/c, p_{zy})_o \\ &= A(\dot{v}/c, p_{zy})_o \end{aligned} \tag{61}$$

or

$$\begin{aligned} (\dot{v}/c)_{n-1} &= A_{11}(\dot{v}/c)_o + A_{12}(p_{zy})_o \\ (p_{zy})_{n-1} &= A_{21}(\dot{v}/c)_o + A_{22}(p_{zy})_o \end{aligned} \tag{62}$$

where A_{ij} are the elements of the matrix A.

The conditions that must be satisfied for free surface waves with no sources at $z = \infty$ are $(p_{zy})_o = 0$ and $V_{2_n} = 0$. This gives

$$A_{21} = -L_n \zeta_n A_{11} \tag{63}$$

This is the Love wave dispersion equation for layered anisotropic media.

In the two layer case $A = a_1$ and equation 63 reduces to

$$\tan k\zeta_1 d_1 = -i \frac{L_2 \zeta_2}{L_1 \zeta_1} \tag{64}$$

as determined directly in Chapter VII. This in turn reduces to the familiar isotropic form when $N = L = \mu$.

Discussion of Love Wave Solution

Although Love waves are surface waves equation 63 contains body wave information. The only SH body wave information we have discarded in arriving at our solution is the wave leaving the last layer in the direction of positive infinity and for surface measurements this does not concern us.

In the long wave limit each a_m becomes

$$a_m = \begin{bmatrix} 1 & 0 \\ 0 & 1 \end{bmatrix} \qquad m = 1, 2, \ldots, n-1$$

Therefore

$$A = \prod_{1}^{n-1} a_m = \begin{bmatrix} 1 & 0 \\ 0 & 1 \end{bmatrix}$$

and the period equation becomes

$$L_n \zeta_n = 0$$

or

$$c = \beta_n$$

Therefore as $kd_m \to 0$, $m = 1, 2, \ldots, n-1$, $c \to \beta_n$, the shear velocity in the half-space.

For the short wave limit put $\zeta_m = i\zeta_m^*$

$$\zeta_m^* = \left(\frac{N}{L}\right)^{1/2} \left(1 - \frac{c^2}{\beta_m^2}\right)^{1/2}$$

Then

$$a_m = \cosh h\zeta_m^* d_m \begin{bmatrix} 1 & -\dfrac{\tanh \zeta_m^* kd_m}{L_m \zeta_m} \\ -L_m \zeta_m \tanh k\zeta_m^* d_m & 1 \end{bmatrix} \tag{65}$$

As $d_m \to 0$, $m = 2, 3, \ldots, n-1$

$$a_m \to \begin{bmatrix} 1 & 0 \\ 0 & 1 \end{bmatrix}$$

and

$$A = \cosh h\zeta_o^* d_o \begin{bmatrix} 1 & -\dfrac{\tanh \zeta_o^* kd_o}{L_o \zeta_o} \\ -L_o \zeta_o \tanh k\zeta_o^* d_o & 1 \end{bmatrix} \tag{66}$$

giving the period equation

$$\tan k\zeta_o d_o = \frac{L_n \zeta_n^*}{L_o \zeta_o^*} \tag{67}$$

as $c \to \beta_o$, $\zeta_o^* \to 0$, and $k\zeta_o d_o = 0, \pi/2, 3\pi/2, \ldots$ Therefore as $d_o \to \infty$, $k\zeta_o d_o$ remains finite and there are an infinite number of modes, or branches, with $c \to \beta_o$ as $kd_o \to \infty$.

Real roots of the general period equation 63 exist only in the range $\beta_1 < c < \beta_n$ and for $L_{m+1}/L_m = 0$ (a free heterogeneous plate). Complex roots might be expected outside of these regions and would correspond to leaky or non-perfect constructive interference.

In field refraction studies using SH waves the slopes of travel time plots would give β_2 but the intercepts would correspond to the

vertically travelling wave or β_1.

Solutions Recast Into Isotropic Form

For convenience we introduce the following anisotropy factor

$$\xi = \frac{N}{L} = \frac{\beta_2^2}{\beta_1^2}$$

which is unity when there is no anisotropy. Then

$$\zeta = \xi^{1/2}\left(\frac{c^2}{\beta_2^2} - 1\right)^{1/2}$$
$$= \xi^{1/2}\tilde{\zeta}$$

in terms of isotropic constants and the anisotropy factor.

Throughout our development ζ appears only in the combination $L\zeta$ and ζd. In the isotropic case the corresponding terms are $\mu\tilde{\zeta}$ and $\tilde{\zeta}d$. We can therefore have complete equivalence if we define a pseudo-rigidity and a pseudo-thickness.

$$\mu' = L\xi^{1/2} = (LN)^{1/2}$$
$$d' = \zeta^{1/2}d = (N/L)^{1/2}d \qquad (68)$$

for each layer. The pseudo-rigidity in the equivalent isotropic case is the geometric mean of the directional rigidities of the anisotropic problem.

The use of these pseudo-parameters makes it possible to use previous Love dispersion numerical data to determine dispersion in layered anisotropic media. For example the convenient curves,

nomograms and tables of Dorman (1959), Sato (1953), Kanai (1951), and Ewing et al. (1957) can be applied to the anisotropic problem. Likewise, computer programs, such as described by Press et al. (1961) for calculation of Love wave dispersion curves in layered isotropic media can be adapted by use of the pseudo-parameters instead of the isotropic parameters to calculate dispersion in layered anisotropic material. Most of the theory developed for isotropic SH and Love wave propagation, including source and amplitude studies can therefore be applied directly to the anisotropic problem.

A further simplification results from the fact that Love wave dispersion is remarkably insensitive to reasonable changes in the rigidity or rigidity gradient which means, if the velocity is unchanged, a lack of sensitivity to density or density gradient. If the rigidity of a whole section is multiplied by a constant factor, such as $\xi^{-1/2}$, the dispersion is unchanged since rigidities occur only in ratios. The effect of a uniform anisotropy, then, is to telescope the whole section, which is the same as telescoping the T (period) axis of the dispersion curve. For non-uniform anisotropies the section is telescoped non-uniformly but the additional effect on rigidities can usually be ignored. Physically, this procedure may be interpreted as changing the travel time in the vertical direction and, therefore, changing the vertical velocity relative to the horizontal which is just the type of anisotropy we have introduced.

Figure 8 shows the effect of uniform anisotropy on Love waves in a simple layered structure. Note that the frequency is proportional to $\xi^{-1/2}$.

Transverse Isotropy As the Limit Of a Layered Solid

Postma (1955) and White and Angona (1955) have shown that, in situations of plane stress or infinite wavelength, a formation consisting of alternating plane parallel isotropic layers of different properties can be regarded as a homogeneous transversely isotropic system. One would expect this correspondence to hold for wavelengths long compared to the individual layer thicknesses. The resulting anisotropy is not as general as that developed in this paper since the inequality $N > L$ must hold for a laminated body, and, of course, the long wavelength restriction can be quite severe. To investigate the range of validity of the above correspondence we will carry out a more general analysis.

Consider a laminated medium made up of alternating layers of two different isotropic materials. A section of the material is then composed of doublets, not necessarily identical in component or total thicknesses. The matrix relating conditions at the top and bottom of each doublet is

$$b_m = a_{m-1}a_m$$

$$= \cos k\tilde{\zeta}_{m-1}d_{m-1}\cos k\tilde{\zeta}_m d_m \begin{bmatrix} 1 & \frac{1}{\mu_{m-1}\tilde{\zeta}_{m-1}}\tan k\zeta_{m-1}d_{m-1} \\ i\mu_{m-1}\tilde{\zeta}_{m-1}\tan k\tilde{\zeta}_{m-1}d_{m-1} & 1 \end{bmatrix}$$

$$\times \begin{bmatrix} 1 & \frac{1}{\mu_m\tilde{\zeta}_m}\tan k\tilde{\zeta}_m d_m \\ i\mu_m\zeta_m\tan k\tilde{\zeta}_m d_m & 1 \end{bmatrix}$$

$$= \cos k\tilde{\zeta}_{m-1}d_{m-1}\cos k\tilde{\zeta}_m d_m$$

$$\times \begin{bmatrix} 1 - \frac{\mu_m\tilde{\zeta}_m}{\mu_{m-1}\tilde{\zeta}_{m-1}}\tan k\tilde{\zeta}_{m-1}d_{m-1}\tan k\tilde{\zeta}_m d_m & \frac{i}{\mu_m\tilde{\zeta}_m}\tan k\tilde{\zeta}_m d_m + \frac{i}{\mu_{m-1}\tilde{\zeta}_{m-1}}\tan k\tilde{\zeta}_{m-1}d_{m-1} \\ i\mu_{m-1}\tilde{\zeta}_{m-1}\tan k\tilde{\zeta}_{m-1}d_{m-1} + i\mu_m\tilde{\zeta}_m\tan k\tilde{\zeta}_m d_m & 1 - \frac{\mu_{m-1}\tilde{\zeta}_{m-1}}{\mu_m\tilde{\zeta}_m}\tan k\tilde{\zeta}_{m-1}d_{m-1}\tan k\tilde{\zeta}_m d_m \end{bmatrix}$$

(69)

Consider now wavelengths long compared to any doublet thickness. Then

$$b_m = \begin{bmatrix} 1 & ik\left(\frac{d_m}{\mu_m} + \frac{d_{m-1}}{\mu_{m-1}}\right) \\ ik(\mu_{m-1}\tilde{\zeta}^2_{m-1}d_{m-1} + \mu_m\tilde{\zeta}^2_m d_m & 1 \end{bmatrix} \tag{70}$$

to order $k\tilde{\zeta}d$. The first neglected term is of order $(k\tilde{\zeta}d)^2$.

To the same order, for a single anisotropic layer

$$a_m = \begin{bmatrix} 1 & \frac{id_m}{L} \\ kiN_m\tilde{\zeta}^2_m d_m & 1 \end{bmatrix} \tag{71}$$

The matrices a_m and b_m are equal, independent of phase velocity if,

$$N = \frac{\mu_{m-1}d_{m-1} + \mu_m d_m}{d}$$

$$L = \frac{\mu_m\mu_{m-1}d}{\mu_{m-1}d_m + \mu_m d_{m-1}} \tag{72}$$

Therefore a doublet or a series of doublets may be replaced by a single anisotropic layer with the above directional properties. These relations are identical with those given by Postma (1955) from purely static considerations. This analysis may be extended in an obvious way to layered media with more than two components. For long wavelengths the whole near surface section may be replaced by an equivalent anisotropic layer. This considerably reduces computa-

tional labor for surface wave studies on multi-layered media.

For a layered solid the directional rigidities L and N are, respectively, the harmonic and arithmetic means of the component rigidities. The effective density is the arithmetic mean of the individual densities. This procedure replaces a layered isotropic structure with a single anisotropic layer. These two structures are equivalent for long wavelengths. If we now form the geometric mean of the directional rigidities and change the thickness of the layer as shown in the previous section we can replace the single anisotropic layer by an equivalent single isotropic layer.

This analysis shows the correct way to average properties when several isotropic layers are replaced by one. Instead of averaging velocities, as has been common practice, we must form the geometric mean of the arithmetic and harmonic means of the rigidities and modify the thickness.

For a material composed of N laminations, each of different rigidity, μ_i, and thickness, d_i, the equivalent single isotropic layer has the following properties

$$\mu' = \left[\frac{\left(\prod_{1}^{N} \mu_i \right)\left(\sum_{1}^{N} d_i \mu_i \right)}{\sum_{1}^{N} \left(d_i \prod_{\substack{1 \\ j \neq i}}^{N} \mu_j \right)} \right]^{1/2} \tag{73}$$

$$d' = \left[\frac{\left(\sum_{1}^{N} d_i \mu_i \right) \sum_{1}^{N} d_i \left(\prod_{\substack{1 \\ j \neq i}}^{N} \mu_j \right)}{\left(\prod_{1}^{N} \mu_i \right)} \right]^{1/2} \tag{74}$$

for

$$k \sum_{1}^{N} d_i \ll 1$$

To illustrate the range of validity of the laminated solid approximation and as an independent check on the theory developed in this paper several numerical examples were computed on the Love wave dispersion program described by Press et al. (1961).

In the first example phase velocities were computed for Love type motion of a laminated (10 layer) plate and for the equivalent homogeneous anisotropic plate. The parameters are taken from Postma (1955) and are tabulated in Tables 2 and 3 under Postma Solid I. The results are shown in Table 4. The difference in period is about 2-1/2% at a wavelength corresponding to about 10 times the thickness of the largest individual layer. The difference gets more pronounced for shorter wavelengths and would get smaller if the laminations were thinner.

In the second example a three layer half-space was constructed as shown in figure 9 corresponding to a layer of Postma Solid I over a layer of Postma Solid II over an isotropic half-space. Dispersion was computed for each surface layer split into 20 laminations and then

Table 2

Parameters for Postma solids (I and II) in arbitrary consistent units

	d_1/d_2				
	I	II	μ	β	ρ
1	1/3	3	2.5	3.04	2.7
2	1	1	0.6	1.62	2.3

Table 3

Parameters for equivalent anisotropic solids

	D	D'	N	L	μ'	β_1	β_2	ρ	ξ
I	1	1.21	1.08	0.74	0.895	1.76	2.12	2.4	1.46
III	1	1.20	2.03	1.40	1.684	2.32	2.79	2.6	1.45

Table 4

Phase Velocity and Period for the fundamental Love mode in anisotropic plate (T_1) and laminated plate (T_2)

C	T_1	T_2
5.0	1.032	1.029
4.6	1.011	1.009
4.2	0.983	0.981
3.8	0.946	0.943
3.4	0.892	0.888
3.0	0.806	0.804
2.6	0.660	0.659

into 40 laminations, and also for the equivalent anisotropic layers. As the number of laminations increases the dispersion converges to the anisotropic case, as shown in figure 9.

Figure 10 shows the displacements as a function of depth for cases A and B, for three values of the phase velocity. The displacements are normalized to the surface value. The effect of the laminations is to keep the particle motion from dying off so rapidly. The displacements for the laminated case diverge more from the anisotropic case as the wavelength gets smaller.

Although theoretical studies of laminated media, viewed as an approximation to an anisotropic solid, have proved useful in shedding light on anisotropic wave propagation problems, the present results can be used the other way around; i.e. replacing complicated layered structures by simple equivalent anisotropic structures. To illustrate, we have constructed a medium consisting of 20 layers having the composite properties of Postma Solid I, overlying an isotropic half-space. The resulting Rayleigh wave dispersion for the first two modes is shown as the solid line in figure 11. The 20 layers can be replaced by a single anisotropic layer, with a large decrease in computing time, which gives the dispersion shown by dashes. There is good agreement over the entire range of the computations. The dotted line is the best single layer isotropic fit to the data.

Comparison With Field Data

Jolly (1956) in a fundamental field study of shear waves demonstrated the existence of transverse isotropy in a near surface section

of shale. He obtained refraction data for SH, SV and P waves and also some Love wave data. There was good evidence to indicate that the horizontal SH velocity was approximately twice the vertical velocity. Figure 12 gives Jolly's experimental results and two theoretical curves. The dashed curve is the predicted dispersion using field refraction and reflection data and assuming isotropy. The anisotropic results are given by the solid curves. Structure parameters are given in the table on figure 12; the isotropic curve has $\xi = 1$ throughout the section. It is obvious that the assumption of isotropy is not warranted. An increase in anisotropy with depth seems to be indicated although the structure determined is not unique.

X. THE GENERAL ANISOTROPIC CASE

We will now derive the equations of motion for an infinite medium with three orthogonal planes of symmetry. This symmetry is general enough to allow specialization to cubic, orthorhombic, tetragonal, trigonal and hexagonal symmetries. A possible application is the propagation of surface waves over a medium acted on by non-isotropic horizontal stresses.

Consider a material which possesses at each point three planes of symmetry at right angles to each other and take these planes as the coordinates x, y and z. This symmetry corresponds to an orthorhombic crystal and has a strain energy function W, given by (Love, 1944),

$$\begin{aligned} 2W = {} & c_{11}e_{xx}^2 + c_{22}e_{yy}^2 + c_{33}e_{zz}^2 + 2c_{12}e_{xx}e_{yy} \\ & + 2c_{13}e_{xx}e_{zz} + 2c_{23}e_{yy}e_{zz} + c_{44}e_{yz}^2 \\ & + c_{55}e_{zx}^2 + c_{66}e_{xy}^2 \end{aligned} \tag{75}$$

where e_{ij} are the strains and c_{ij} are the nine elastic constants required to describe the material.

The stress equations of motion are three of the following form, involving the displacements u, v, w and the stresses p_{ij},

$$\rho \frac{\partial^2 u}{\partial t^2} = \frac{\partial p_{xx}}{\partial x} + \frac{\partial p_{xy}}{\partial y} + \frac{\partial p_{xz}}{\partial z} \tag{76}$$

where

$$p_{ij} = \frac{\partial W}{\partial e_{ij}} \tag{77}$$

We obtain the displacement equations of motion by substituting 77 into 76. This yields the following three equations,

$$\begin{aligned}
\rho\ddot{u} &= c_{11}\frac{\partial^2 u}{\partial x^2} + c_{55}\frac{\partial^2 u}{\partial z^2} + c_{66}\frac{\partial^2 u}{\partial y^2} + (c_{13}+c_{55})\frac{\partial^2 w}{\partial x \partial z} \\
&\quad + (c_{12}+c_{66})\frac{\partial^2 v}{\partial x \partial y} \\
\rho\ddot{v} &= c_{66}\frac{\partial^2 v}{\partial x^2} + c_{22}\frac{\partial^2 v}{\partial y^2} + c_{44}\frac{\partial^2 v}{\partial z^2} + (c_{66}+c_{12})\frac{\partial^2 u}{\partial x \partial y} \\
&\quad + (c_{23}+c_{44})\frac{\partial^2 w}{\partial y \partial z} \\
\rho\ddot{w} &= c_{33}\frac{\partial^2 w}{\partial z^2} + c_{44}\frac{\partial^2 w}{\partial y^2} + c_{55}\frac{\partial^2 w}{\partial x^2} + (c_{55}+c_{13})\frac{\partial^2 u}{\partial x \partial z} \\
&\quad + (c_{23}+c_{44})\frac{\partial^2 v}{\partial z \partial y}
\end{aligned} \tag{78}$$

These are the equations of motion for an infinite orthorhombic medium. We will confine ourselves temporarily to the case where motion takes place in the two dimensions x, z so that $v = \frac{\partial}{\partial y} = e_{yy} = e_{xy} = e_{yz} = 0$. The equations 78 become,

$$\begin{aligned}
\rho\ddot{u} &= c_{11}\frac{\partial^2 u}{\partial x^2} + c_{55}\frac{\partial^2 u}{\partial z^2} + (c_{13}+c_{55})\frac{\partial^2 w}{\partial x \partial z} \\
\rho\ddot{w} &= c_{33}\frac{\partial^2 w}{\partial z^2} + c_{55}\frac{\partial^2 w}{\partial x^2} + (c_{55}+c_{13})\frac{\partial^2 u}{\partial x \partial z}
\end{aligned} \tag{79}$$

For an isotropic body $c_{11} = c_{22} = c_{33} = n + 2\mu$, $c_{12} = c_{13} = n$, $c_{44} = c_{55} = c_{66} = \mu$ and the above equations reduce to the familiar form. For waves propagated in a direction given by the direction cosines (ℓ, o, m) assume u, w to vary as $\exp\{ik(\ell x + nz - ct)\}$. Substitution of these forms into 79 and setting the determinate equal to zero gives the wave velocity equation,

$$(c_{11}\ell^2 + c_{55}n^2 - \rho c^2)(c_{55}\ell^2 + c_{33}n^2 - \rho c^2) - (n\ell)^2(c_{13} + c_{55})^2 = 0 \quad (80)$$

A wave travelling in the x-direction has $\ell = 1$, $n = 0$ and the solutions to the velocity equation are

$$c^2 = \frac{c_{11}}{\rho}, \quad \frac{c_{55}}{\rho} \quad (81)$$

For an isotropic material these correspond respectively to the compressional and shear velocities. Particle motion has been constrained to the xz plane, therefore the shear velocity corresponds to SV motion.

In the z-direction, $\ell = 0$, $n = 1$ and

$$c^2 = \frac{c_{33}}{\rho}, \quad \frac{c_{55}}{\rho} \quad (82)$$

The compressional motion is now controlled by the elastic constant c_{33}. Therefore P-waves in the x- and z-directions travel at different velocities but the SV waves travel at the same velocity. At intermediate directions we still have two solutions to 80 but neither is purely compressional or purely shear type motion. Information about the elastic constant c_{13} must be obtained from an intermediate

angle in the xz-plane.

For Rayleigh type waves we consider

$$(u, w) = [\, U(z), W(z)]\, e^{i(\omega t - kx)}$$

Substitution into the equations of motion gives

$$\begin{aligned} -\rho\omega^2 U(z) &= -c_{11}k^2 U(z) - ik(c_{13}+c_{55})W'(z) + c_{55}U''(z) \\ -\rho\omega^2 W(z) &= c_{33}W''(z) - ik(c_{55}+c_{13})U'(z) - k^2 c_{55}W(z) \end{aligned} \tag{83}$$

This is identical to the equations derived for Rayleigh wave propagation along the x-direction in transversely isotropic media with c_{55} replacing c_{44}. From the form of the above equations it is clear that a similar correspondence holds for the z- and y-directions so that for these directions the theory developed in previous sections applies directly. We are therefore in a position to treat surface waves propagating along, or perpendicular to, directions of principle stress or "regional grain."

XI. TWO-DIMENSIONAL MODEL SEISMOLOGY WITH DIRECTIONAL VELOCITIES

Introduction

The use of two-dimensional seismic models has played an important role in the study of wave propagation problems since its introduction in 1954. Oliver et al. (1954) demonstrated by use of Love's concept of "generalized plane stress" (Love, 1944) that the two-dimensional isotropic equations of motion are exactly equivalent to the three-dimensional equations when the body velocities are replaced by the corresponding plate velocities. Therefore since the boundary conditions are also of the same form any three-dimensional problem involving body or surface wave propagation and particle motion in a single plane in infinite, semi-infinite, or layered isotropic solid media can be modeled exactly in two-dimensions. Healy and Press (1960) extended the theory to include continuous velocity depth and density functions and described the fabrication of appropriate models.

This section generalizes the theory to anisotropic media.

Plate Theory

Consider a free plate in the xz plane, with the y axis perpendicular to it. The stresses p_{yy} vanish throughout the plate and the tangential stresses p_{yz}, p_{yx} vanish on the faces. The equations of motion are now

$$\frac{\partial p_{xx}}{\partial x} + \frac{\partial p_{zx}}{\partial x} = \rho \ddot{u}$$

$$\frac{\partial p_{zx}}{\partial x} + \frac{\partial p_{zz}}{\partial z} = \rho \ddot{w} \tag{84}$$

For waves long compared to the plate thickness we set $p_{yy} = 0$ in equation 77 and obtain

$$e_{yy} = -\frac{1}{c_{22}} \left(c_{23} \frac{\partial w}{\partial z} + c_{12} \frac{\partial u}{\partial x} \right) \tag{85}$$

With this substitution in p_{xx}, p_{zz} of equation 77 we obtain for the plate equations of motion, for an orthorhombic plate,

$$\left(\frac{c_{11}c_{22} - c_{12}^2}{c_{22}} \right) \frac{\partial^2 u}{\partial x^2} + c_{55} \frac{\partial^2 u}{\partial z^2} + \left(\frac{c_{55}c_{22} - c_{12}c_{23} + c_{13}c_{12}}{c_{22}} \right) \frac{\partial^2 w}{\partial x \partial z} = \rho \ddot{u}$$

$$\left(\frac{c_{33}c_{22} - c_{23}^2}{c_{22}} \right) \frac{\partial^2 w}{\partial z^2} + c_{55} \frac{\partial^2 w}{\partial x^2} + \left(\frac{c_{55}c_{22} + c_{13}c_{22} - c_{23}c_{12}}{c_{22}} \right) \frac{\partial^2 u}{\partial x \partial z} = \rho \ddot{w} \tag{86}$$

This is of the same form as equation 79 with the following replacements,

$$c_{11} \rightarrow \frac{c_{11}c_{22} - c_{12}^2}{c_{22}}$$

$$c_{33} \rightarrow \frac{c_{33}c_{22} - c_{23}^2}{c_{22}}$$

$$(c_{13} + c_{55}) \rightarrow \frac{c_{55}c_{22} + c_{13}c_{22} - c_{23}c_{12}}{c_{22}}$$

$$c_{55} \rightarrow c_{55}$$

Using techniques similar to those employed in the preceding sections we may show that the plate velocities, C_p, in the x-direction are

$$C_p^2 = \frac{c_{11}c_{22} - c_{12}^2}{c_{22}} \quad , \quad \frac{c_{55}}{\rho} \tag{87}$$

and in the z-direction are

$$C_p^2 = \frac{c_{33}c_{22} - c_{23}^2}{c_{22}} \quad , \quad \frac{c_{55}}{\rho} \; . \tag{88}$$

Note that the plate shear velocities are the same as the infinite media shear velocities.

Consider now a thin orthorhombic plate which occupies the xz plane from $z = 0$ to $z = +\infty$.

At the free edge we will have "edge" waves, which correspond to the surface waves over a half-space, by requiring

$$p_{xz} = p_{zz} = 0 \quad \text{at} \quad z = 0$$

These conditions may be written,

$$c_{55}\left(\frac{\partial u}{\partial z} + \frac{\partial w}{\partial x} \right) = 0 \tag{89}$$

$$\left(c_{13} - \frac{c_{23}c_{12}}{c_{22}}\right) \frac{\partial u}{\partial x} + \left(c_{33} - \frac{c_{23}^2}{c_{22}} \right) \frac{\partial w}{\partial z} = 0 \tag{90}$$

Choose plane wave solutions of the form

$$u = Ue^{i(\omega t - kx)}\, e^{\nu_i z}$$
$$w = We^{i(\omega t - kx)}\, e^{\nu_i z} \tag{91}$$

Substitution into the equations of motion gives

$$-\rho w^2 U = -c_{11}k^2 U + c_{22}\nu_i^2 U - (c_{13} + c_{55})ik\nu_i W$$
$$-\rho w^2 W = c_{22}\nu_1^2 W - c_{55}k^2 W - (c_{55} + c_{13})ik\nu_i U \tag{92}$$

Consistency requires

$$(\rho w^2 - c_{11}k^2 + c_{55}\nu_i^2)(\rho w^2 - c_{55}k^2 + c_{33}\nu_i^2) + k^2\nu_i^2(c_{13} + c_{55})^2 = 0 \tag{93}$$

This is a quadratic in ν_i^2 and is identical in form to the expression derived earlier (Equation 13) for ν_i^2 in a transversely isotropic layer with c_{55} replacing c_{44}.

Applying the edge conditions we get the period equation

$$\Pi_1\Gamma_2 - \Gamma_1\Pi_2 = 0 \tag{94}$$

where

$$\Pi_1 = \nu_1 + k\gamma_1 \qquad \Pi_2 = \nu_2 + k\gamma_2$$
$$\Gamma_1 = c_{13}'k - \gamma_1\nu_1 c_{33}' \qquad \Gamma_2 = c_{13}'k - \nu_2\gamma_2 c_{33}'$$

and

$$c_{13}' = \frac{c_{13}c_{22} - c_{23}c_{12}}{c_{22}}$$

$$c_{33}' = \frac{c_{33}c_{22} - c_{23}^2}{c_{22}}$$

This is the period equation of Rayleigh waves propagated along the edge of an orthorhombic plate.

This is identical with the equation for Rayleigh waves along the surface of a transversely isotropic solid (Anderson, 1961) with the exception that the plate elastic constants replace the regular constants. Similar correspondence holds in more complicated problems.

Thus, anisotropic problems can be modelled two-dimensionally. By replacing all directional body velocities by the corresponding directional plate velocities the general anisotropic theory can be applied to two-dimensional models.

With the help of M. Nafi Toksoz a model experiment was performed on an aluminum plate which was grooved in order to make it anisotropic. The measured directional plate and Rayleigh velocities are tabulated in Table 5. The Rayleigh velocities computed on the basis of equation 94 are also tabulated. They agree, within experimental error, with those measured. Also the horizontal and vertical shear velocities are the same, as predicted by theory.

Table 5

MEASURED AND COMPUTED DIRECTIONAL VELOCITIES ON GROOVED ALUMINUM PLATE

	Measured (in./μsec.)	Computed (in./μsec.)
$a_p(0^o)$	0.208	
$a_p(90^o)$	0.173	
$\beta_p(0^o)$	0.106	
$\beta_p(90^o)$	0.107	
$C_R(0^o)$	0.1017	0.0993
$C_R(90^o)$	0.100	0.0982

XII. EVIDENCE FROM LONG PERIOD SURFACE WAVES

Introduction

Long period surface waves have proved invaluable for providing information about average crustal and mantle structures over the entire path traversed. In particular they can be used to determine structure in areas inaccessible to standard body wave analyses such as ocean basins. The recent advent of high speed computing techniques and the introduction of long-period seismographs have made this method even more valuable for determining structures over paths of oceanic and continental dimensions. While these advances have made it possible, among other things, to verify the existence of Gutenberg's low velocity channel, an inconsistency has been uncovered which is outside the limits of error of the present high precision of the method.

Figure 13 gives observed Love and Rayleigh dispersion for both group and phase velocity over oceanic paths. The theoretical curves were computed on the IBM 7090 with a program described by Press et al. (1961). The structure 8099 was found by Dorman et al. (1960) to give a good fit to the observed Rayleigh wave data and at the same time was consistent with body wave data. When we compute the Love wave dispersion, however, we note a large disagreement between theory and data. The flat portion of the group velocity curve fails to attain the G-wave velocity of 4.4 km/sec.

For such long wavelengths curvature of the earth and gravity cannot be ignored. Bolt and Dorman (1961), and Pekeris et al. (1961)

have computed the free modes of a spherical gravitating earth for several earth models. To estimate the correction necessary to calculations based on flat lying layers we have computed the dispersion for the plane layer equivalent models for the spherical models of the above authors and derived a velocity correction as a function of period. This correction is then assumed to be approximately the same for other similar models of the earth.

The results are shown as dashed lines in figure 13. The effect is in the right direction to give better agreement at long periods for Rayleigh group velocities. The Rayleigh phase velocity curve, however, fits the data less well now than previously for the plane layer approximation. This means that the actual structure must have lower velocities than assumed, at least to explain the Rayleigh data. The effect on Love wave group velocities is slight. The velocities appear to be too low to explain the Love wave data. Thus, curvature and gravity alone do not seem capable of resolving the discrepancy.

Figure 14 shows data from continental paths and the theoretical curves computed on the basis of body wave velocities determined by Lehmann (Dorman et al., 1960). The Rayleigh curve is above the data while the Love curve is quite a bit below the corresponding data. Velocities determined by Gutenberg give similar results. The structures of both Gutenberg and Lehmann include a low-velocity zone in the upper mantle.

Landisman and Sato (Dorman et al., 1960) propose a structure called 38-XII which they claim gives a good fit to continental Love data.

Their actual numerical results were never published so we have computed Love dispersion for this model. Figure 15 shows the results and the corresponding Rayleigh dispersion computed by Dorman et al. This model fits Love data fairly well and the Rayleigh data not at all.

With the earth models proposed to date it seems we cannot simultaneously satisfy body, Rayleigh and Love wave data.

One thing is unsatisfactory about all of the preceding theoretical results. The density distribution that has been used, namely Bullen A, is based on Jeffrey's velocity structure and is therefore inconsistent with the actual velocities used. It might be assumed that the density distribution will affect Love and Rayleigh dispersion differently and therefore, with proper densities, the discrepancy may be removed.

Figure 16 shows five density distributions that have been proposed by various authors. All of these are based, to some extent, on seismic velocities. Bullen A has been used in most previous investigations. Bullen B and Bullard are similar and probably represent an upper bound on possible densities in the upper mantle. Although these density distributions have been shown by Birch (1961a) to be internally inconsistent we have computed dispersion based on them to get an idea of the effect of an extreme density variation. The curve labelled Gutenberg-Birch was computed by Birch (1961) on the basis of Gutenberg's velocities. Miki's (1956) results are very close to the Gutenberg-Birch values. Instead of using a universal depth-density distribution we use the velocity-density relation com-

puted by Birch to convert compressional velocities to densities. The Birch models therefore have densities consistent with the velocities used to determine them. It turns out that the Birch densities give dispersion that for all practical purposes is the same as Bullen A.

The effect of density on dispersion of Rayleigh waves is shown in figure 17. Clearly the Bullen B and Bullard densities are unsatisfactory. This conclusion has already been reached by MacDonald and Ness (1961) on the basis of free oscillation data and Birch (1961) on other grounds. The Gutenberg-Birch values give dispersion indistinguishable on this scale from that of Bullen A. In figure 18 are shown the results for both Love and Rayleigh for density distributions of Bullen A and Bullard. The velocity structure is Gutenberg's throughout. While we have destroyed the good Rayleigh fit we have hardly affected Love dispersion. Therefore, the density assumptions do not seem to be responsible for the Love Rayleigh disagreement.

Another alternative is anisotropy. Since SH velocities control Love wave dispersion and SV velocities control Rayleigh wave dispersion we would not expect a single shear velocity structure to explain both types of waves if the earth is anisotropic.

Starting with model 8099 we perturbed the horizontal SH velocity to obtain the best fit to both Love phase and group velocity data. The final structure so determined is shown in figure 19 as CIT 2. 8099 then gives the horizontal SV velocity and CIT 2 gives the horizontal SH velocity.

The fundamental and first higher Love modes are shown in figure 20. The group velocity is relatively flat from 30 to 250 secs.

as we know it should be from the pulse nature of the G-wave. The fundamental has a maximum of 4.38 km./sec. at a period of about 50 seconds--this is the G-wave velocity determined from world circling waves. It has a minimum of 4.35 km./sec. at a period of about 190 secs. All the energy in a G-wave in the period band 15-250 seconds arrives in the velocity range 4.35 - 4.38 km./sec. thereby giving the G-wave its pulse-like character. Although still not perfect this is the best fit to date. The shear velocity anisotropy is about 5% in the low velocity zone. A somewhat higher anisotropy is indicated for a better fit to the data.

The first higher Love mode is plotted as a dashed line. The group velocity shows a plateau at 4.4 km./sec. in the period range 15-30 seconds. The S_a phase has just these properties. Therefore the same SH structure explains both the G and S_a waves as similar phenomena associated with different modes.

In figure 21 we show the effect of an anisotropic low velocity zone on the dispersion of Rayleigh waves. $\varphi = 0.8$ corresponds to a compressional wave anisotropy of about 9% throughout the low-velocity zone. If we now apply the spherical earth correction we obtain an excellent fit to both phase and group velocity. Therefore an 8-10% anisotropic low-velocity zone removes the discrepency between Love and Rayleigh waves, explains the S_a phase and improves the previously good fit to the Rayleigh data.

An additional bit of evidence should be quoted here. Vvedenskaya and Balakina (1959) found anomalous values for amplitudes

of SH waves compared to SV and P waves for rays penetrating to the depths of 250-500, 900-1000, 1200-1300, 1800 and 2200 kilometers. They attribute this to a polarization of the transverse waves during double refraction in anisotropic layers of the earth mantle corresponding to the above depths. This presumed anisotropy is particularly pronounced at the depth of the low velocity zone in the upper mantle.

Possible Explanations of Anisotropy

It is well known that non-hydrostatic stresses will cause initially isotropic solids to become anisotropic. The fact that we have earthquakes down to 700 km. seems to imply that non-uniform stresses are being built up and released at least to this depth. The magnitude of this effect can be computed with the help of equations developed by Biot (1940). He showed that a transversal plane wave propagating in the horizontal direction in a material under an initial horizontal stress σ_{11} will propagate at a velocity

$$\beta_2 = (\mu_o + \tfrac{1}{2}(\sigma_{11} - \sigma_{22}))^{1/2}/\rho^{1/2}$$

The vertically travelling wave will have the velocity

$$\beta_1 = (\mu_o - \tfrac{1}{2}(\sigma_{11} - \sigma_{22})^{1/2})/\rho^{1/2}$$

where μ_o is the rigidity of the unstressed material. Therefore

$$\xi = \frac{N}{L} = \frac{\mu_o + \frac{1}{2}(\sigma_{11} - \sigma_{22})}{\mu_o - \frac{1}{2}(\sigma_{11} - \sigma_{22})}$$

If we take $\mu_o = 7 \times 10^{11}$ dy/cm^2 as the rigidity in the low velocity zone then we require a stress difference of about 7×10^{10} dy/gm^2 to give us a 5% velocity anisotropy. This far exceeds the strength of rocks at this depth which is usually taken as not more than 10^9 dy/cm^2.

A non-uniform stress field in itself, therefore, cannot be responsible for an anisotropy as high as 10% unless the strength of rocks at the depth of the low velocity zone is greater than presently thought.

Non-hydrostatic stresses, however, can have a more subtle indirect effect. They can cause reorientation and alignment of crystals by recrystallation, plastic flow, and mechanical rotation. These processes would be particularly effective at the high temperatures thought to exist in the low velocity zone. A crystalline material that has been exposed to non-hydrostatic stresses for a sufficient period of time will have the constituent minerals aligned. The minerals must themselves be anisotropic if the alignment is to lead to overall anisotropy. Therefore existence of anisotropy at depth requires both non-hydrostatic stresses and the presence of strongly anisotropic minerals. Thus anisotropy gives evidence both for the nature of the stresses and the composition in a given zone of the earth.

Table 6 gives the average minimum anisotropy of several common rocks under 10 kb. confining pressure as given by Birch (1961). The anisotropies measured represent lower bounds since the samples were oriented at random. The appreciable anisotropy found for dunites is in striking contrast to igneous rocks in general. A similar conclusion can be drawn from work of S. Katz (personal communication). It

is interesting to note that the ratio of the highest compressional velocity to that of the lowest found on single specimens of dunite is almost exactly that found by Verma (1960) on single crystals of olivine, the primary constituent of dunite. This suggests that there is almost 100% orientation of the crystals in dunite. That there is a preferred orientation of crystals in most dunites can be demonstrated by the usual optical methods. In fact the theory and applications of this paper form a crude seismic analogy to the methods used in optical petrology.

If the upper mantle does indeed prove to be about 8-10% anisotropic upon more detailed examination, then this is a strong argument with our present knowledge of rock anisotropies for a dunitic composition. More rocks must be tested in the laboratory before other compositions can be ruled out. In any event, the presence or absence of anisotropy is a powerful new tool for defining the properties of rocks at depth.

In addition to non-uniform stresses, convection currents and directional heat flow could also cause orientated crystal growth and reorientation.

Table 6

Rock (10 kb.)*	Anisotropy (ϕ_{min})	Number of Samples
Pyroxenites	0.94	4
Dunites	0.86	7
Serpentinites	0.89	3
Quartzite	0.94	1
Gneisses	0.93	3

* Birch (1961)

REFERENCES

Alterman, Z., H. Jarosch and C. L. Pekeris, Propagation of Rayleigh waves in the earth, Geoph. Jour., 4, 219-241, 1961.

Aki, K. and F. Press, Upper mantle structure under oceans and continents from Rayleigh waves, Geoph. Jour. Roy. Astr. Soc., 5, 292-305, 1961.

Anderson, D. L., Elastic wave propagation in layered anisotropic media, J. Geoph. Res., v. 66, 2953-2963, 1961.

*Arkhangel'skaya, V. M., Dispersion of surface waves and crustal structure, Bull. Acad. Sci., USSR, Geoph. Ser., 1360-1391,

*Arkhangel'sky, V. T., D. P. Kirnos, I. I. Popov and V. N. Solov'ev, Observations of long-period seismic waves at the Simferopol station, Bull. Acad. Sci., USSR, Geoph. Ser., 5, 670-675, 1961.

*Bath, M., and A. L. Arroyo, Attenuation and dispersion of G waves, Jour. Geoph. Res. (in press).

*Ben-Menahem, A. and M. Nafi Tokzos, (personal communication), 1961.

Biot, M., The influence of initial stress on elastic waves, Jour. Appl. Phy., 11, 522-530, 1940.

Birch, F., Composition of the earth's mantle, Geoph. Jour. Roy. Astr. Soc., 4, 295-311, 1961a.

Birch, F., The velocity of compressional waves in rocks to 10 kilobars, Part 2, Jour. Geoph. Res., 66, 2199-2224, 1961b.

Bolt, B. and J. Dorman, Phase and group velocities of Rayleigh waves in a spherical, gravitating earth, Jour. Geoph. Res., 66, 2965-2981, 1961.

*Brune, J. N., H. Benioff and M. Ewing, Long-period surface waves from the Chilean Earthquake of May 22, 1960, recorded on linear strain seismographs, Jour. Geoph. Res., 66, 2895-2910, 1961.

Dorman, J., Numerical solutions for Love wave dispersion on a half-space with double surface layer, Geophysics, 24, 12-29, 1959.

*Dorman, J., M. Ewing, and J. Oliver, Study of shear velocity distribution in the upper mantle by mantle Rayleigh Waves, Bull. Seismol. Soc. Amer., 50, 87-115, 1960.

*Ewing, W. M., W. S. Jardetzky and F. Press, Elastic waves in layered media, McGraw-Hill, New York, 1957.

*Ewing, M. and F. Press (see data published in Dorman et al., 1960).

Gassman, F., Elastic waves through a packing of spheres, Geophysics, 16, 673-685, 1951.

Gutenberg, B., Physics of the earth's interior, Academic Press, New York, 1959.

Harkrider, D. G. and D. L. Anderson, Computation of surface wave dispersion for multilayered anisotropic media, Bull. Seism. Soc. Amer. (in press).

Haskell, N. A., Dispersion of surface waves on multi-layered media, Bull. Seism. Soc. Amer., 43, 17-34, 1953.

Healy, J. and F. Press, Two-dimensional seismic models with continuously variable velocity depth and density functions, Geophysics, 25, 987-997, 1960.

Helbig, K., Elastiche Wellen in anisotropen Medien, Gerlands Beitrage zur geophysik, 67, 177-211, 256-288, 1958.

Jolly, R.N., Investigation of shear waves, Geophysics, 21, 905-938, 1956.

Kanai, K., On the group velocity of dispersive surface waves, Bull. Earthquake Res. Inst. (Tokyo), 29, 49-60, 1951.

Knopoff, L., On Rayleigh wave velocities, Bull. Seism. Soc. Amer., 42, 307-308, 1952.

*Kovach, R., Surface wave dispersion for an Asio-African and a Eurasian Path, Jour. Geoph. Res., 64, 805-813, 1959.

Layet, C., A. C. Clement, G. Pommier, and A. Buffet, Some technical aspects of refraction seismic prospecting in the Sahara, Geophysics, 26, p. 437-446, 1961.

Love, A. E. H., A treatise on the mathematical theory of elasticity, 4th ed., reprinted by Dover Publications, New York, 1944.

MacDonald, G. F. and N. Ness, A Study of the free oscillations of the earth, Jour. Geoph. Res., 66, 1865-1911, 1961.

Mason, W. P., Physical Acoustics and the properties of solids, Bell Laboratory series, D. Van Nostrand Co., Inc., Princeton, N.J., 1958.

Miki, H., On the earth's mantle, Mem., Coll. Soc., U. Kyoto, 27, Ser. A, 363-403, 1956.

Musgrave, M. J. P., The propagation of elastic waves in crystals and other anisotropic media, Reports on Progress in Physics, 22, 74-96, 1959.

Oliver, J., Frank Press and M. Ewing, Two-dimensional model seismology, Geophysics, 19, 202-219, 1954.

Phinney, R. A., Leaking modes in the crustal waveguide, part I: The oceanic PL wave, Geophys. Research (in press) 1961.

Postma, G. W., Wave propagation in a stratified medium, Geophysics, 20, 780-806, 1955.

Press, F., and M. Ewing, Propagation of elastic waves in a floating ice sheet, Trans. Am. Geophys. Union, 32, 673-678, 1951.

Press, F., D. Harkrider, and C. A. Seafeldt, A fast convenient program for computation of surface wave dispersion curves in multilayered media, Bull. Seism. Soc. Am. (in press), 1961.

Satô, Y., Rayleigh waves projected along the plane surface of a horizontally isotropic and vertically acolotropic elastic body, Bull. Earthquake Research Inst. (Tokyo) 28, 23-30, 1950.

Satô, Y., Study on surface waves. II: Velocity of surface waves propagated from elastic plates, Bull. Earthquake Research Inst. (Tokyo), 29, 223-261, 1951.

Satô, Y., Study on surface waves, VIII, Bull. Earthquake Res. Inst. (Tokyo), 31, 81-87, 1953.

* Satô, Y., Attenuation, dispersion, and the wave guide of the G wave, Bull. Seism. Soc. Am., 48, 231-251, 1958.

Satô, Y., M. Landisman and M. Ewing, Love waves in a heterogeneous spherical earth, Jour. Geoph. Res., 65, 2399-2404, 1960.

Stoneley, R., The seismological implications of acolotropy in Continental structure, Monthly Notices Roy. Astron. Soc.: Geophys. Suppl. 5, 222-232, 1949.

Tolstoy, I., Wave propagation in elastic plates; low and high mode dispersion, J. Acoust. Soc. Amer., 29, 37-42, 1957.

Uhrig, L. F. and F. A. Van Melle, Velocity anisotropy in stratified media, Geophysics, 20, 774-779, 1955.

Verma, R. K., Elasticity of some high-density crystals, Jour. Geoph. Res., 65, 747-766, 1960.

Vvedenskaya, A. V. and L. M. Balakina, Double refraction in the earth's mantle, Bull. Acad. Sci., USSR, Geoph. Ser., 1138-1146, 1959.

White, J. E. and R. L. Sengbush, Velocity measurements in near-surface formations, Geophysics, 18, 54-69, 1953.

White, J. E. and F. A. Angona, Elastic wave velocities in laminated media, J. Acoust. Soc. Am., 27, 310-317, 1955.

*Sources of data for figures 13, 14, 15, 17, 20 and 21.

LIST OF CAPTIONS

Figure

1. Effect of anisotropy on M_{11} in a transversely isotropic plate.
2. Range of existence of M_{11} through M_{22} for $1/4 < \sigma < 1/2$ in isotropic plates and location of corresponding modes for anisotropic plates.
3. Dispersion in a free anisotropic plate with the properties of ice.
4. Dispersion in a laminated plate.
5. Geometry of the layered situation under investigation.
6. Existence diagram for Rayleigh waves in multilayered anisotropic media for different Poisson type assumptions. In region I $c_{13} \approx c_{33} - 2c_{44}$. In region II $c_{13} \approx c_{11} - 2c_{44}$. The area below the pertinent curve is forbidden to Rayleigh waves.
7. Velocity surface of SH waves in a transversely isotropic medium.
8. The effect of a uniform anisotropy on Love wave dispersion in a simple layered structure.
9. Dispersion of Love waves in a system composed of two anisotropic surface layers overlying an isotropic half-space, and comparison with the laminated case.
10. Horizontal displacements versus depth for cases A (anisotropic) and B (laminated).
11. Dispersion of Rayleigh waves in a system composed of a single layer of Postma Solid I overlying an isotropic half-space for modes M_{11} and M_{21}.
12. Isotropic and anisotropic dispersion data compared with field results of Jolly (1956). The structure parameters in the table closely approximate refraction results.
13. Experimental and theoretical group and phase velocity determinations for long period Love and Rayleigh waves. Large circles are Love data; small circles are Rayleigh data. Data for this and following figures are from starred entries in References.

Figure

14. Group velocity data and theory for Love and Rayleigh waves over continental paths. The theoretical curve is for the structure determined by Lehmann (Dorman et al., 1960) from body waves.

15. Continental Love and Rayleigh data compared with theoretical curves determined on the basis of model 38-XII of Landisman and Sato (Dorman et al., 1960).

16. Density distributions due to various authors. See Birch (1961), Miki (1956) and Gutenberg (1960).

17. Effect of density on group velocity of long period Rayleigh waves. The spherical earth theoretical computations are due to Bolt and Dorman (1961).

18. Effect of density on dispersion of Love and Rayleigh waves.

19. Shear velocity structure giving best fit for both Rayleigh and Love dispersion. 8099 gives SV velocities; CIT 2 gives horizontal SH velocities.

20. Love wave dispersion for first two modes for structure of CIT 2.

21. Effect of an anisotropic low velocity zone on dispersion of long period Rayleigh waves. The effect of a spherical earth is to move the phase velocity curve for $\varphi = 0.8$ onto the data and improve slightly the fit of the $\varphi = 0.8$ group velocity curve to the data (see Fig. 13).

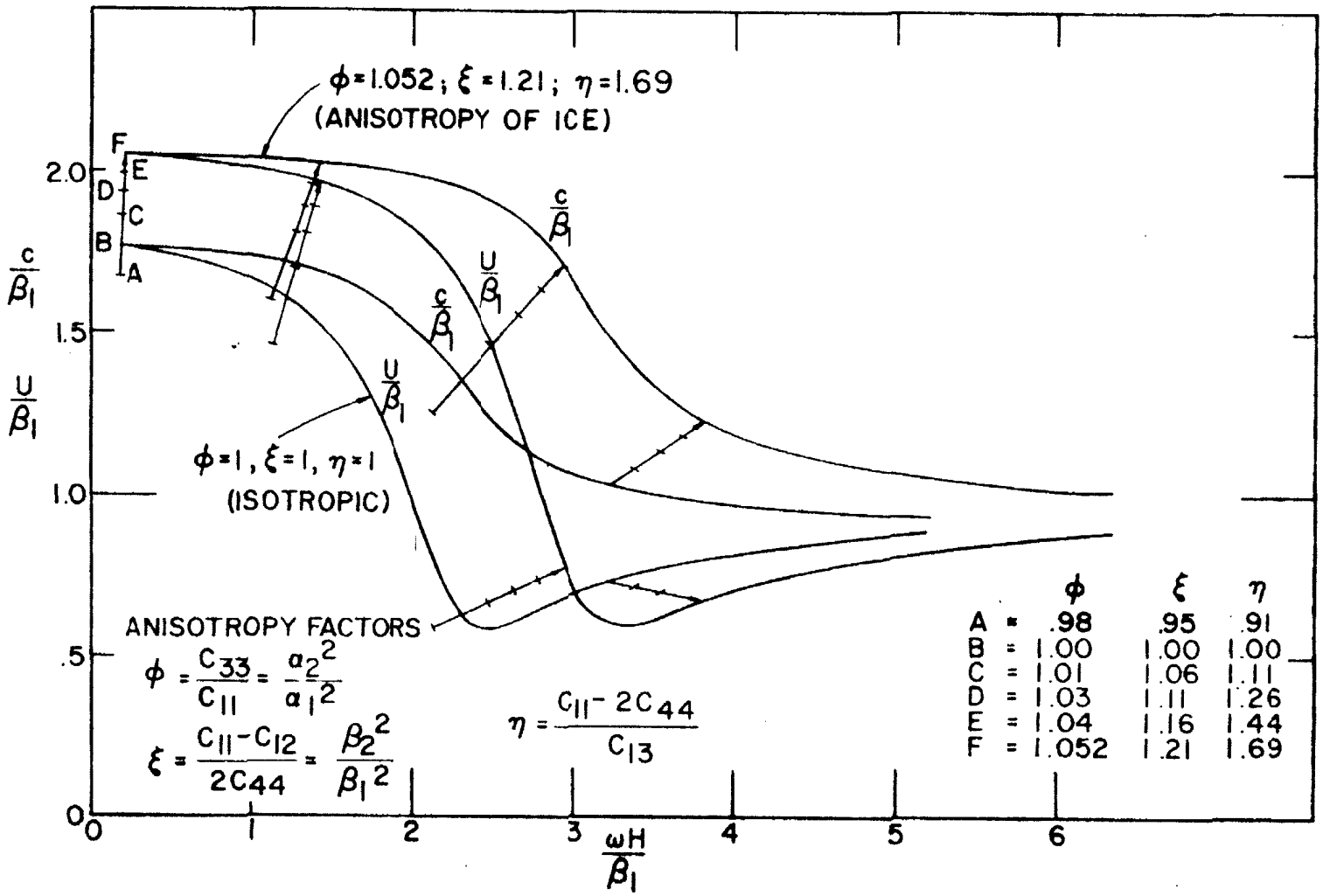
ϕ=1.052; ξ=1.21; η=1.69
(ANISOTROPY OF ICE)
F
E
D
C
B
A
$\frac{c}{\beta_1}$
$\frac{U}{\beta_1}$
ϕ=1, ξ=1, η=1
(ISOTROPIC)
2.0
1.5
1.0
.5
0
0
1
2
3
4
5
6
$\frac{\omega H}{\beta_1}$
ANISOTROPY FACTORS
$\phi = \frac{C_{33}}{C_{11}} = \frac{\alpha_2^2}{\alpha_1^2}$
$\xi = \frac{C_{11}-C_{12}}{2C_{44}} = \frac{\beta_2^2}{\beta_1^2}$
$\eta = \frac{C_{11}-2C_{44}}{C_{13}}$
ϕ ξ η
A = .98 .95 .91
B = 1.00 1.00 1.00
C = 1.01 1.06 1.11
D = 1.03 1.11 1.26
E = 1.04 1.16 1.44
F = 1.052 1.21 1.69

FIG. 1

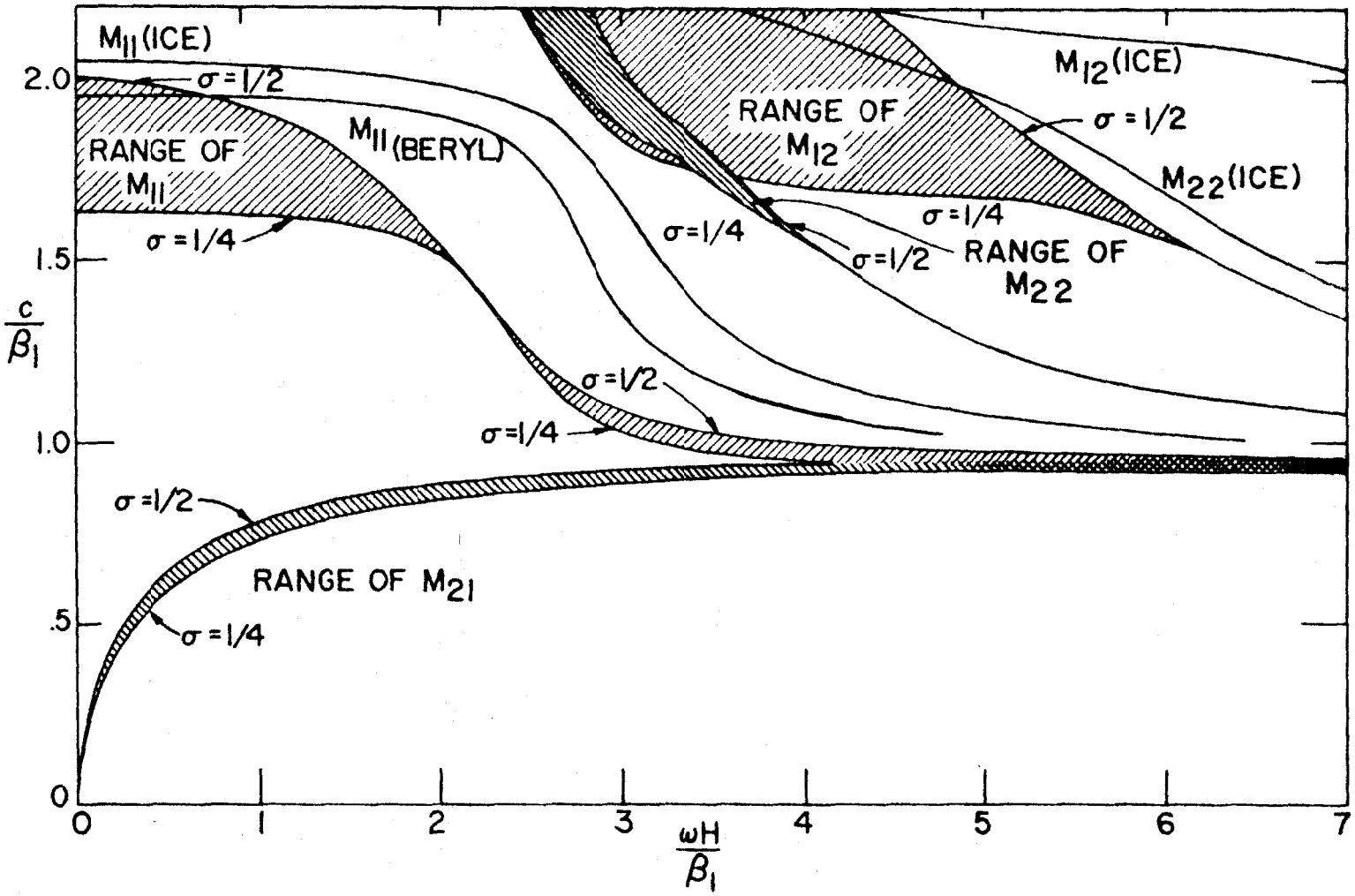
M_{11}(ICE)
σ=1/2
RANGE OF M_{11}
M_{11}(BERYL)
σ=1/4
σ=1/4
σ=1/2
σ=1/4
RANGE OF M_{21}
σ=1/4
M_{12}(ICE)
σ=1/2
RANGE OF M_{12}
σ=1/4
σ=1/2
RANGE OF M_{22}
M_{22}(ICE)
2.0
1.5
1.0
.5
0
$\frac{c}{\beta_1}$
0
1
2
3
4
5
6
7
$\frac{\omega H}{\beta_1}$

FIG. 2

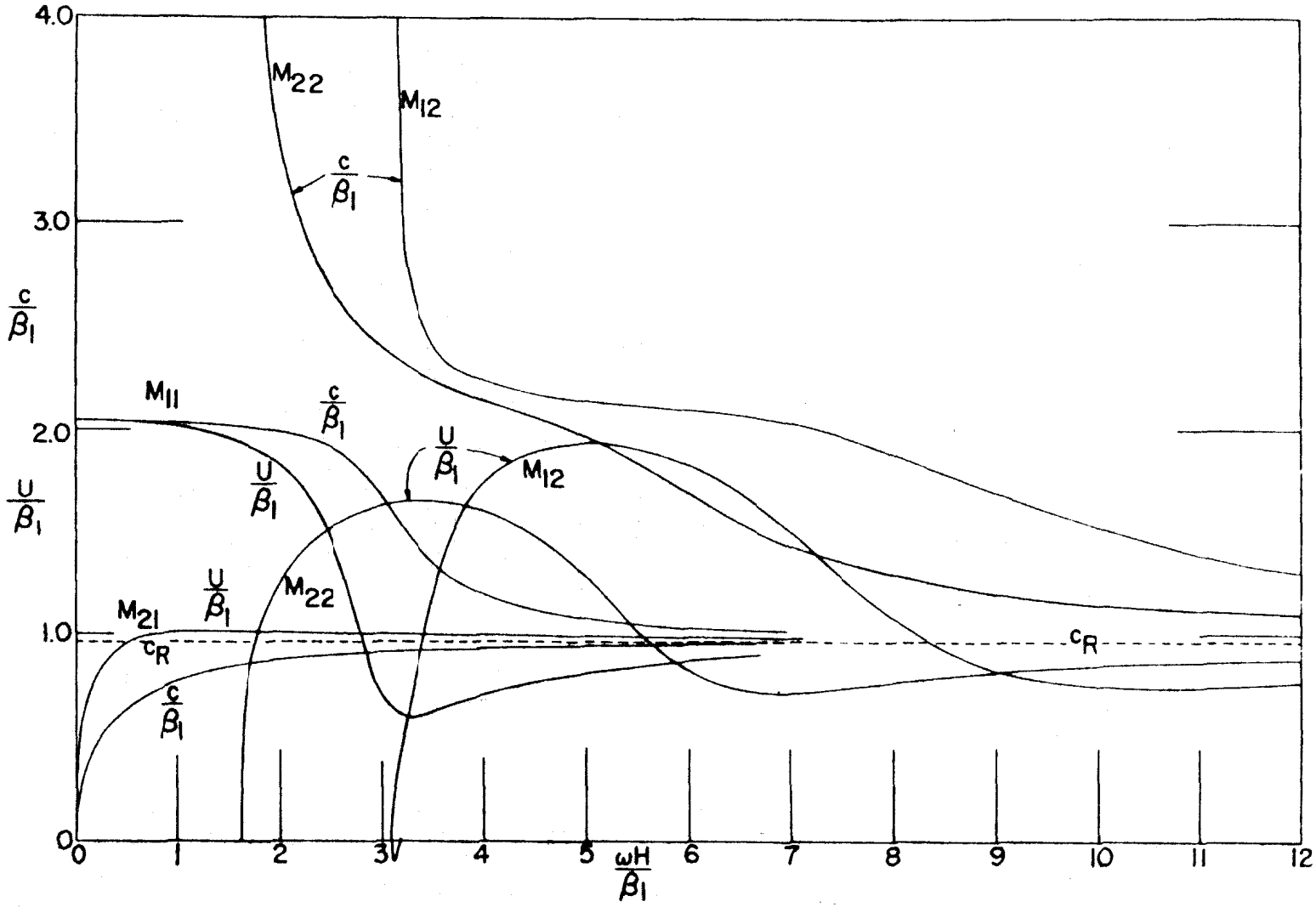
4.0
3.0
2.0
1.0
0
c/β1
U/β1
M22
M12
c/β1
M11
c/β1
U/β1
U/β1
M12
U/β1
M22
M21
cR
c/β1
cR
0
1
2
3
4
5
ωH/β1
6
7
8
9
10
11
12

FIG. 3

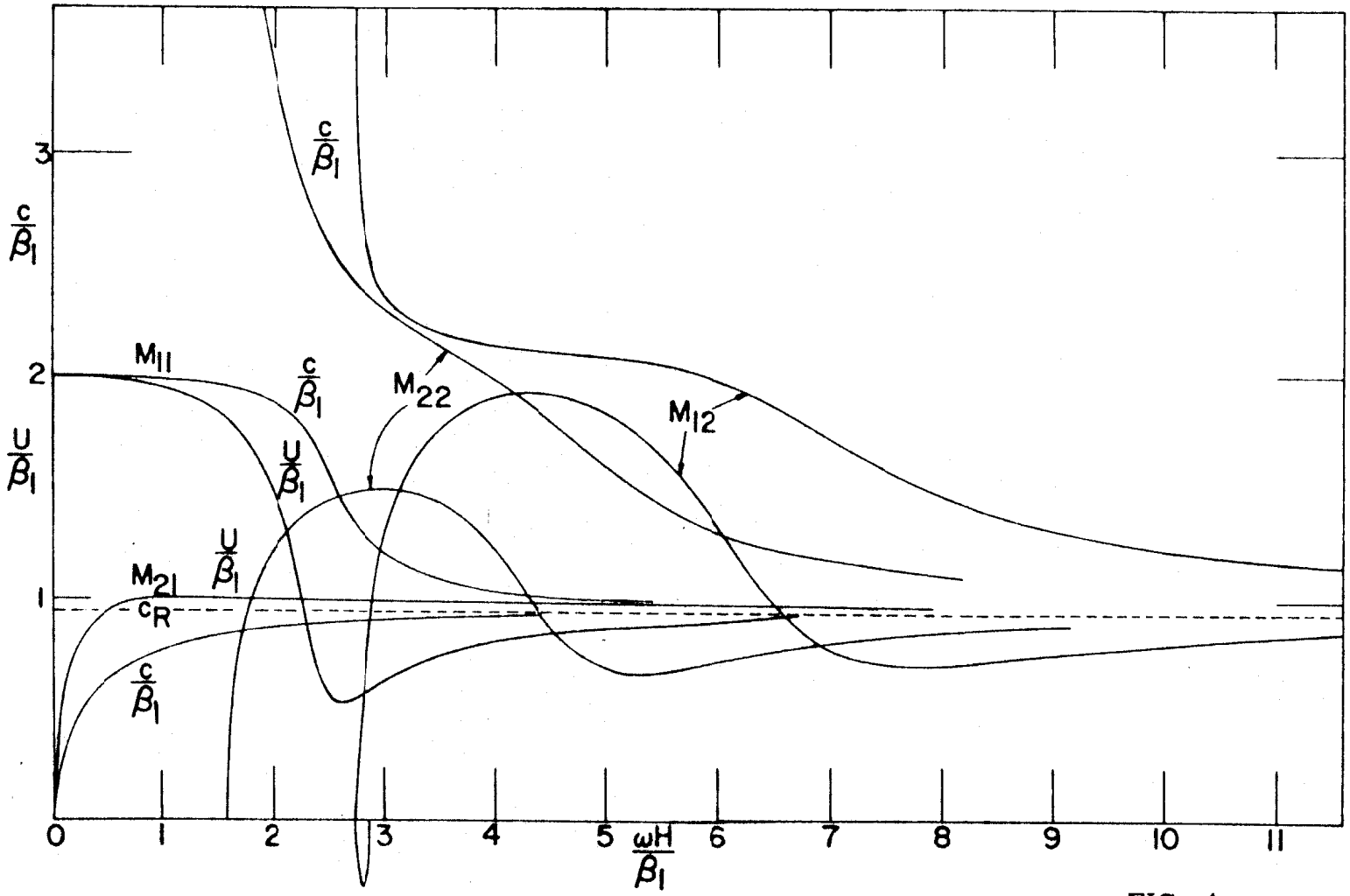

FIG. 4

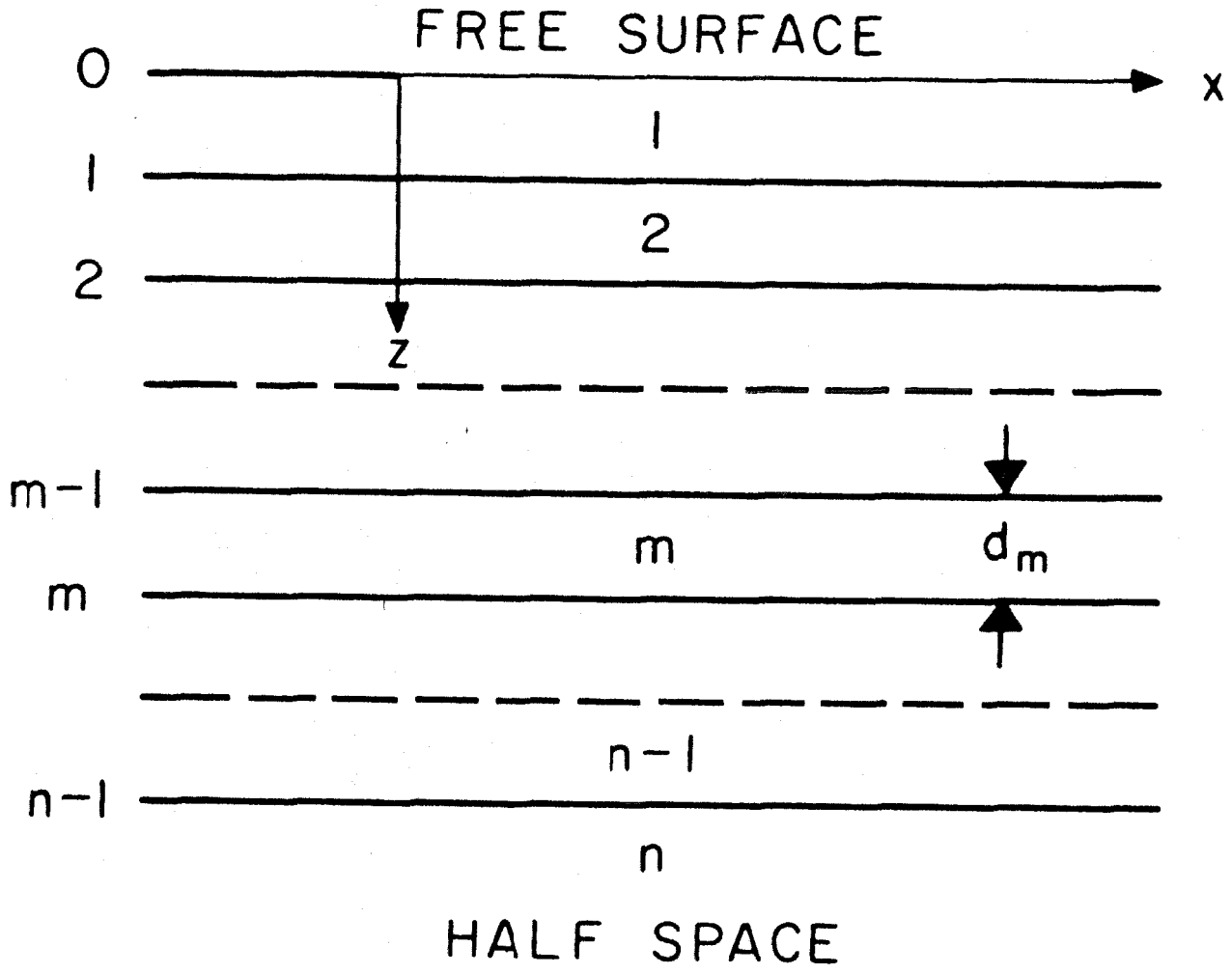

FIG. 5

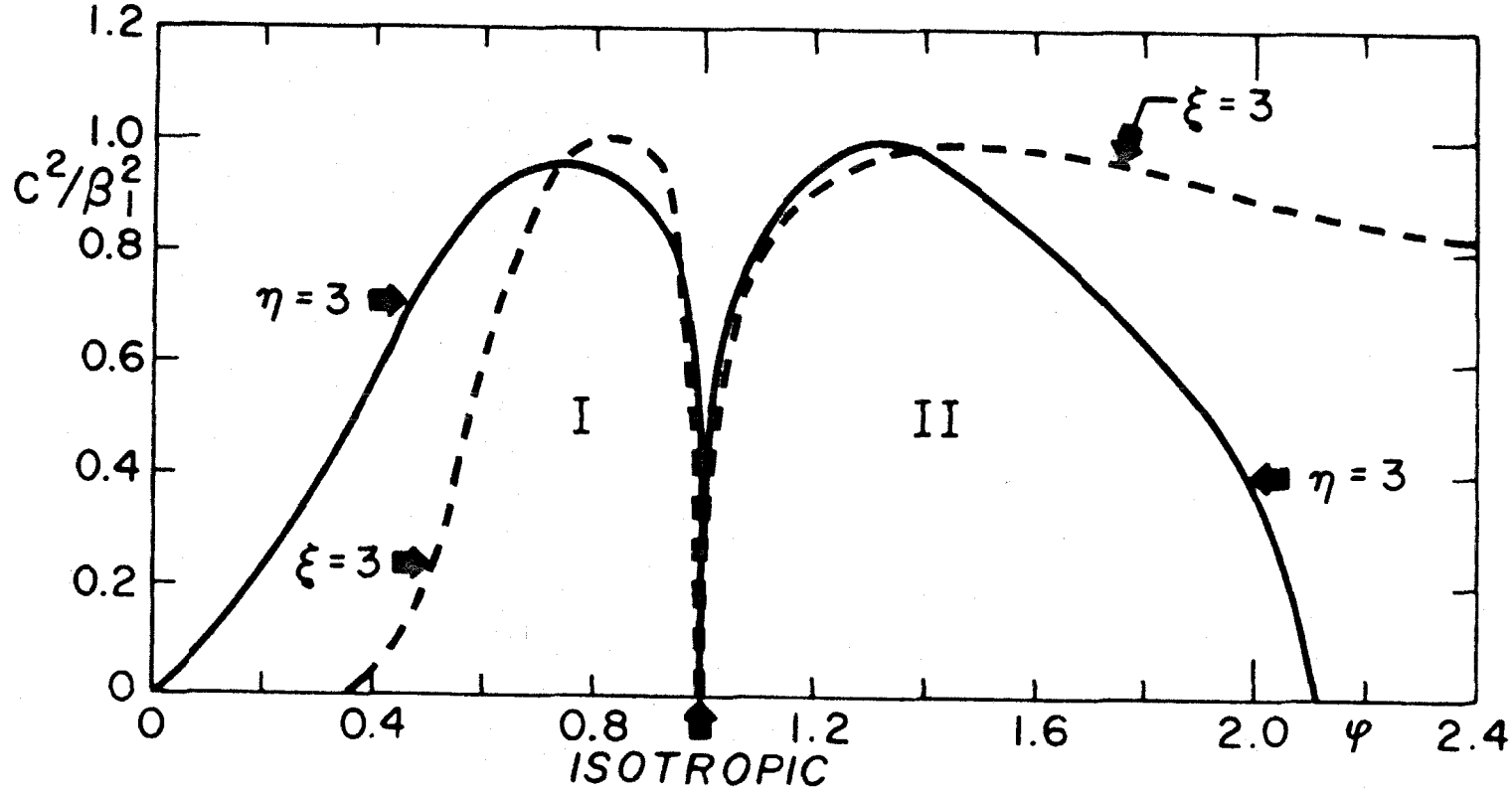

RANGE OF EXISTENCE OF NON-COMPLEX ν

$\xi = \frac{C_{11}}{C_{44}}$; $\eta = \frac{C_{33}}{C_{44}}$; $\phi = \frac{C_{11}}{C_{33}}$

FIG. 6

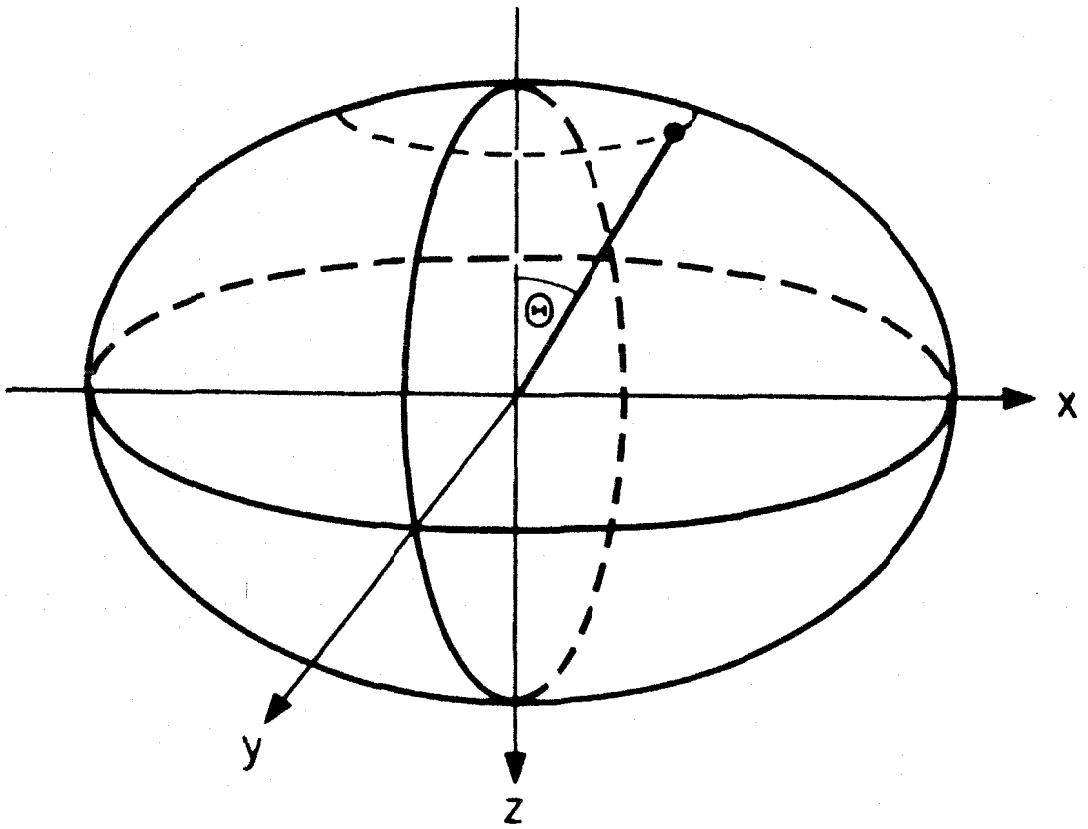

VELOCITY SURFACE

$$\rho\beta^2 = N\sin^2\Theta + L\cos^2\Theta$$

FIG. 7

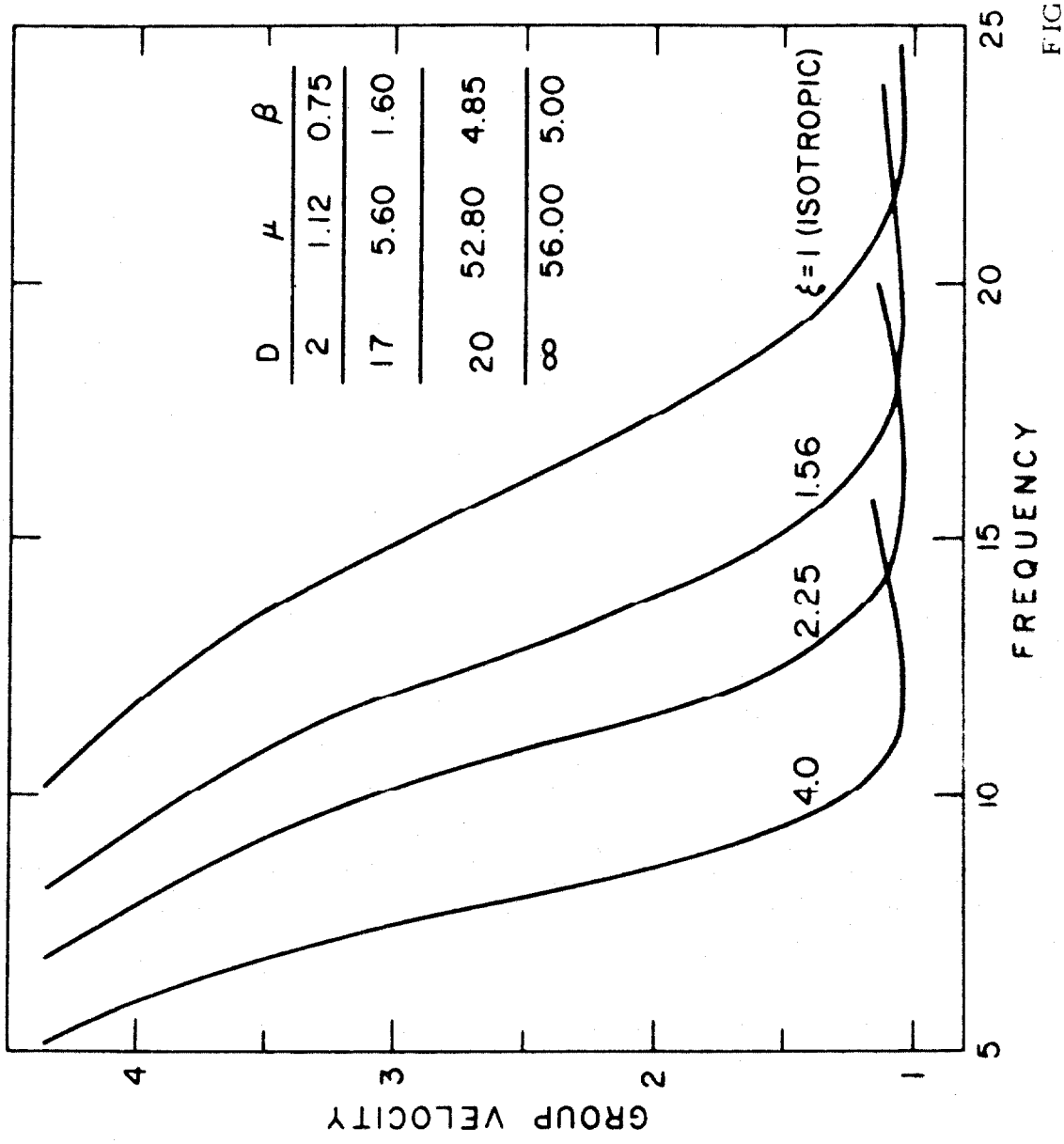
GROUP VELOCITY
FREQUENCY
4
3
2
1
5
10
15
20
25
D
μ
β
2
1.12
0.75
17
5.60
1.60
20
52.80
4.85
∞
56.00
5.00
ξ=1 (ISOTROPIC)
1.56
2.25
4.0

FIG. 8

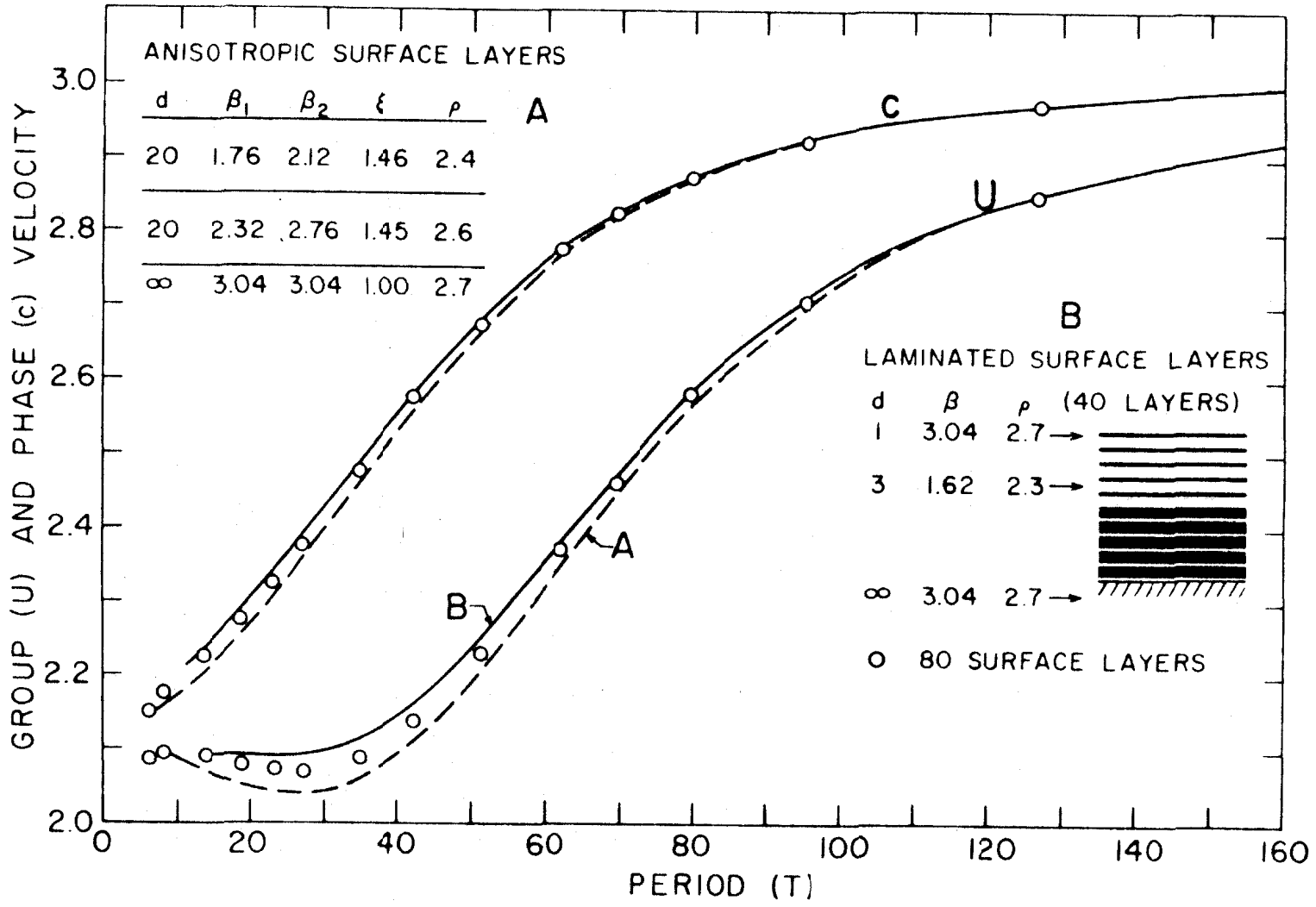
ANISOTROPIC SURFACE LAYERS
d β1 β2 ξ ρ
A
20 1.76 2.12 1.46 2.4
20 2.32 2.76 1.45 2.6
∞ 3.04 3.04 1.00 2.7
C
U
B
LAMINATED SURFACE LAYERS
d β ρ (40 LAYERS)
1 3.04 2.7
3 1.62 2.3
∞ 3.04 2.7
80 SURFACE LAYERS
A
B
GROUP (U) AND PHASE (c) VELOCITY
PERIOD (T)
3.0
2.8
2.6
2.4
2.2
2.0
0
20
40
60
80
100
120
140
160

FIG. 9

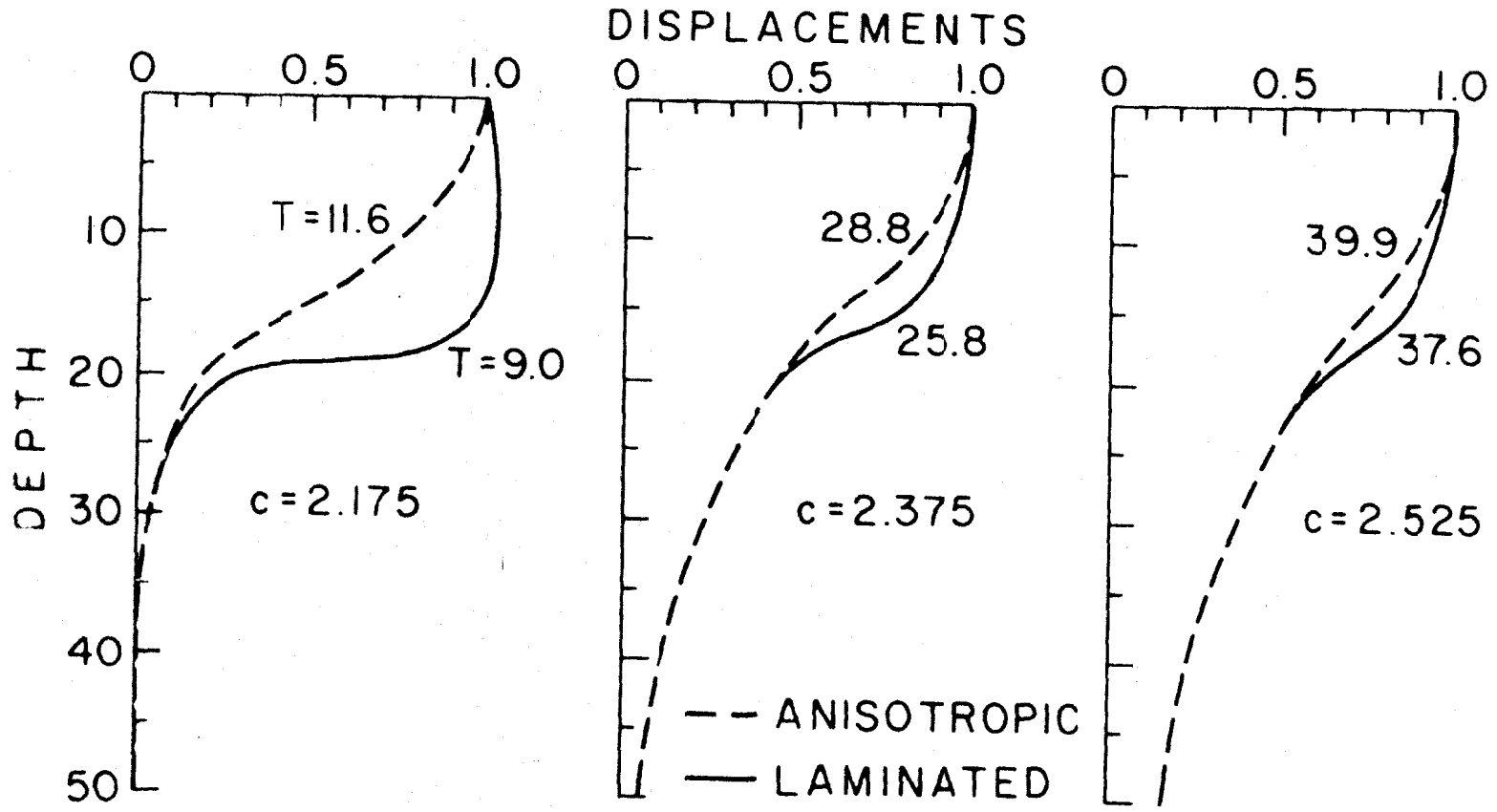
DISPLACEMENTS
0
0.5
1.0
DEPTH
10
20
30
40
50
T=11.6
T=9.0
c=2.175
28.8
25.8
c=2.375
39.9
37.6
c=2.525
ANISOTROPIC
LAMINATED

FIG. 10

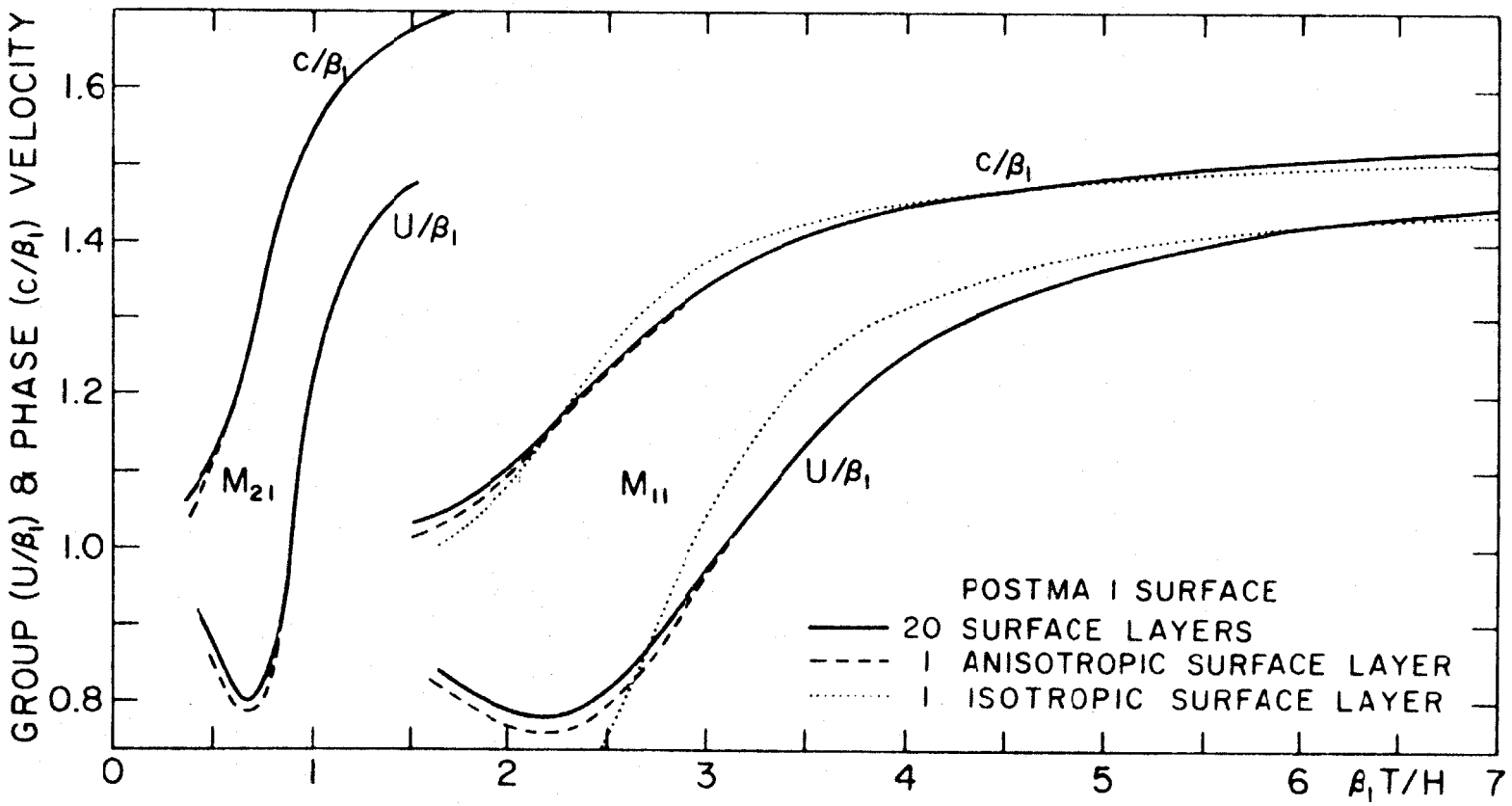
GROUP (U/β1) & PHASE (c/β1) VELOCITY
1.6
1.4
1.2
1.0
0.8
0
1
2
3
4
5
6
7
β1T/H
c/β1
U/β1
M21
M11
POSTMA I SURFACE
20 SURFACE LAYERS
1 ANISOTROPIC SURFACE LAYER
1 ISOTROPIC SURFACE LAYER

FIG. 11

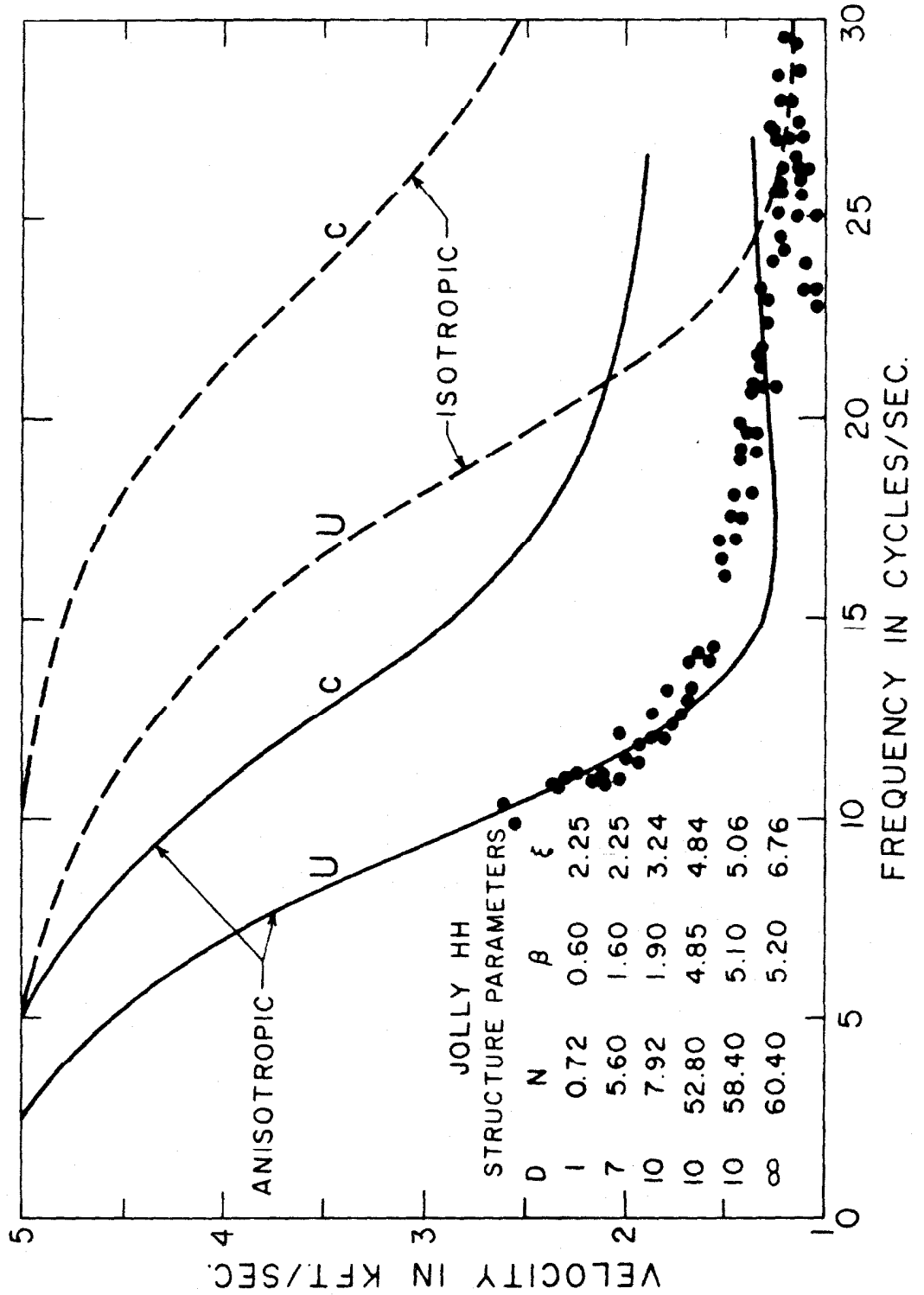
VELOCITY IN KFT/SEC.
FREQUENCY IN CYCLES/SEC.
ISOTROPIC
ANISOTROPIC
U
C
JOLLY HH
STRUCTURE PARAMETERS
D N β ξ
1 0.72 0.60 2.25
7 5.60 1.60 2.25
10 7.92 1.90 3.24
10 52.80 4.85 4.84
10 58.40 5.10 5.06
∞ 60.40 5.20 6.76

FIG. 12

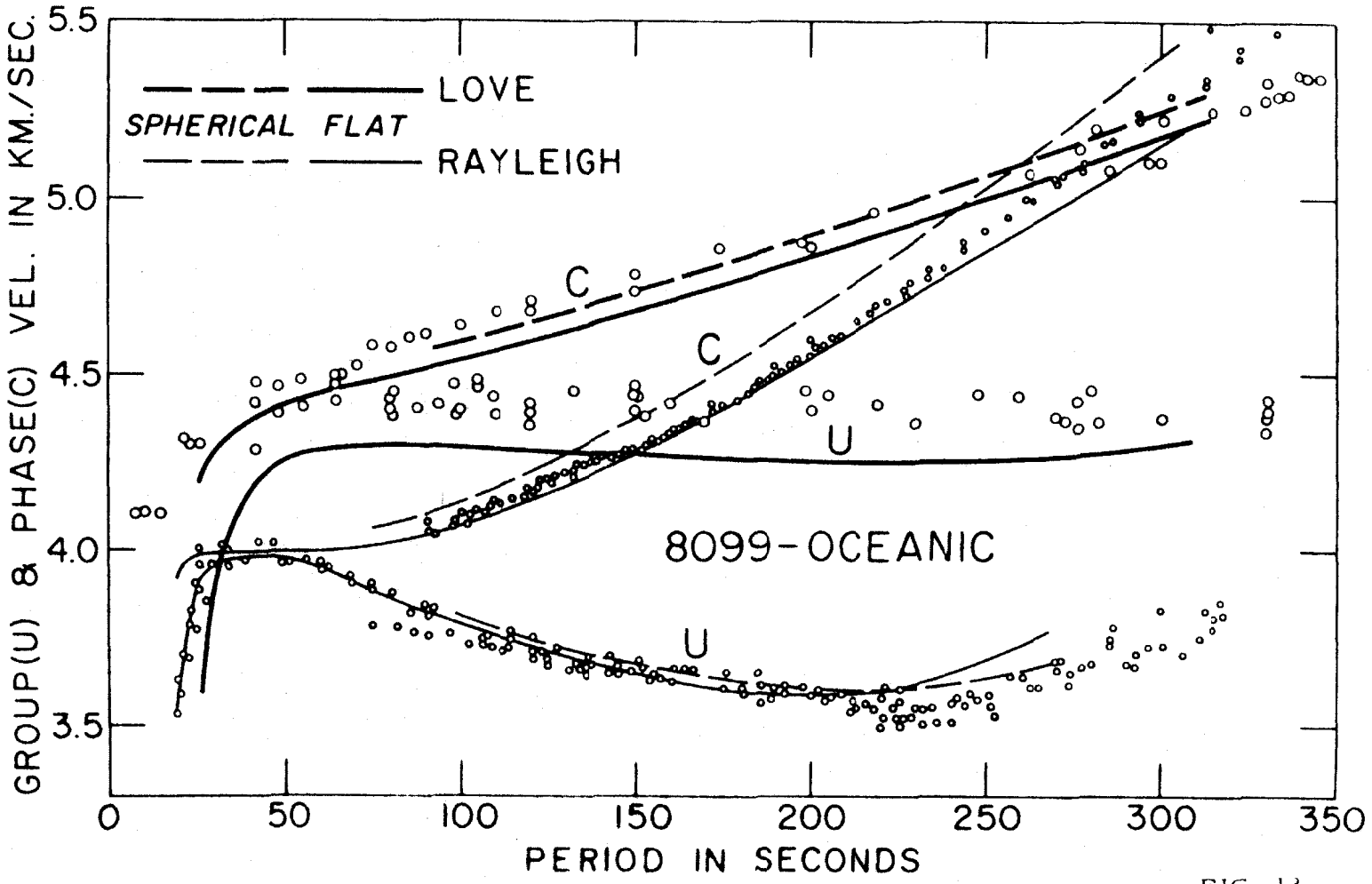
GROUP(U) & PHASE(C) VEL. IN KM./SEC.
5.5
5.0
4.5
4.0
3.5
LOVE
SPHERICAL FLAT
RAYLEIGH
C
C
U
U
8099-OCEANIC
0
50
100
150
200
250
300
350
PERIOD IN SECONDS

FIG. 13

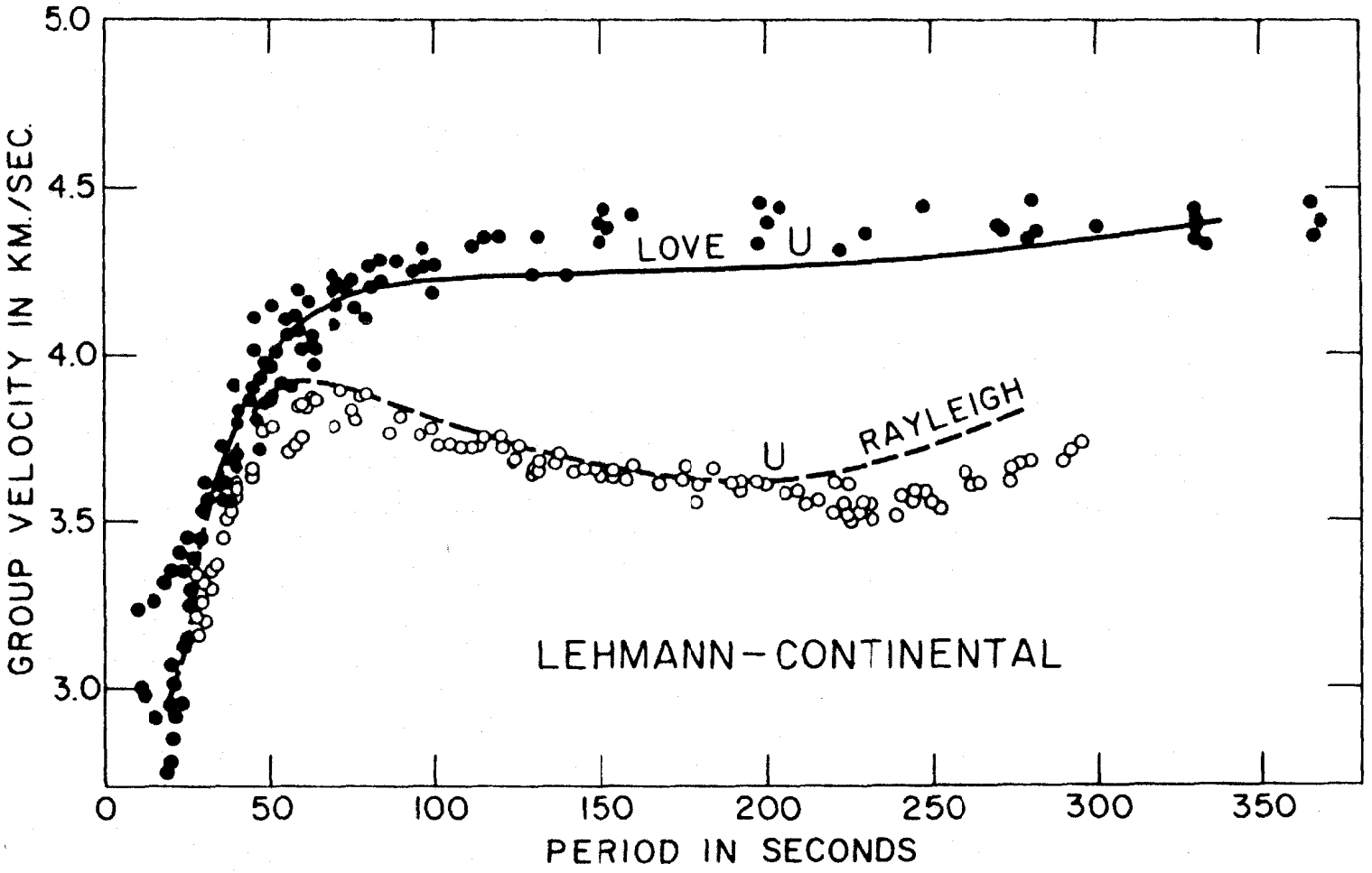
5.0
4.5
4.0
3.5
3.0
GROUP VELOCITY IN KM./SEC.
LOVE U
U RAYLEIGH
LEHMANN-CONTINENTAL
0
50
100
150
200
250
300
350
PERIOD IN SECONDS

FIG. 14

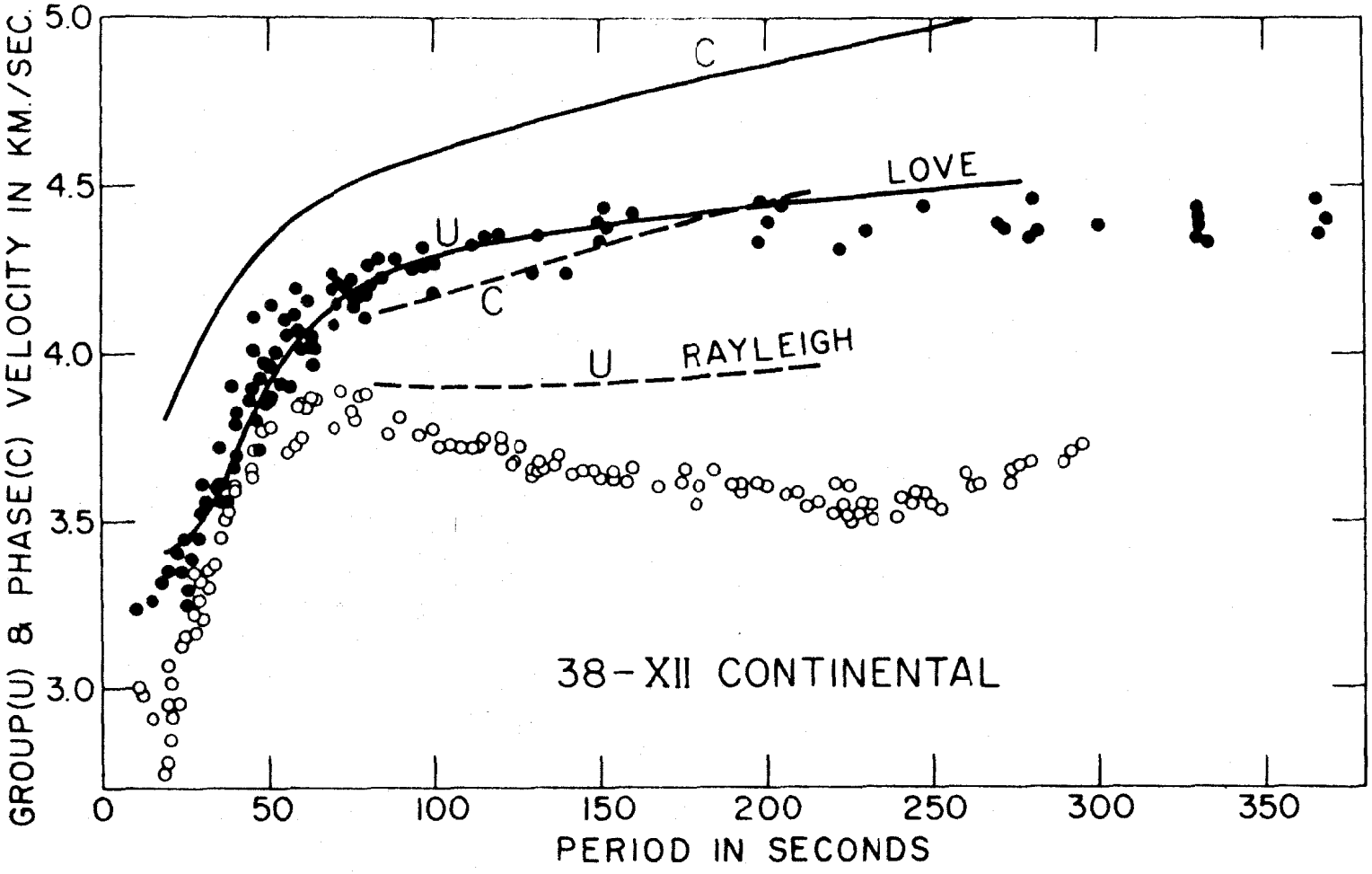
GROUP(U) & PHASE(C) VELOCITY IN KM./SEC.
5.0
4.5
4.0
3.5
3.0
C
LOVE
U
C
U RAYLEIGH
38-XII CONTINENTAL
0
50
100
150
200
250
300
350
PERIOD IN SECONDS

FIG. 15

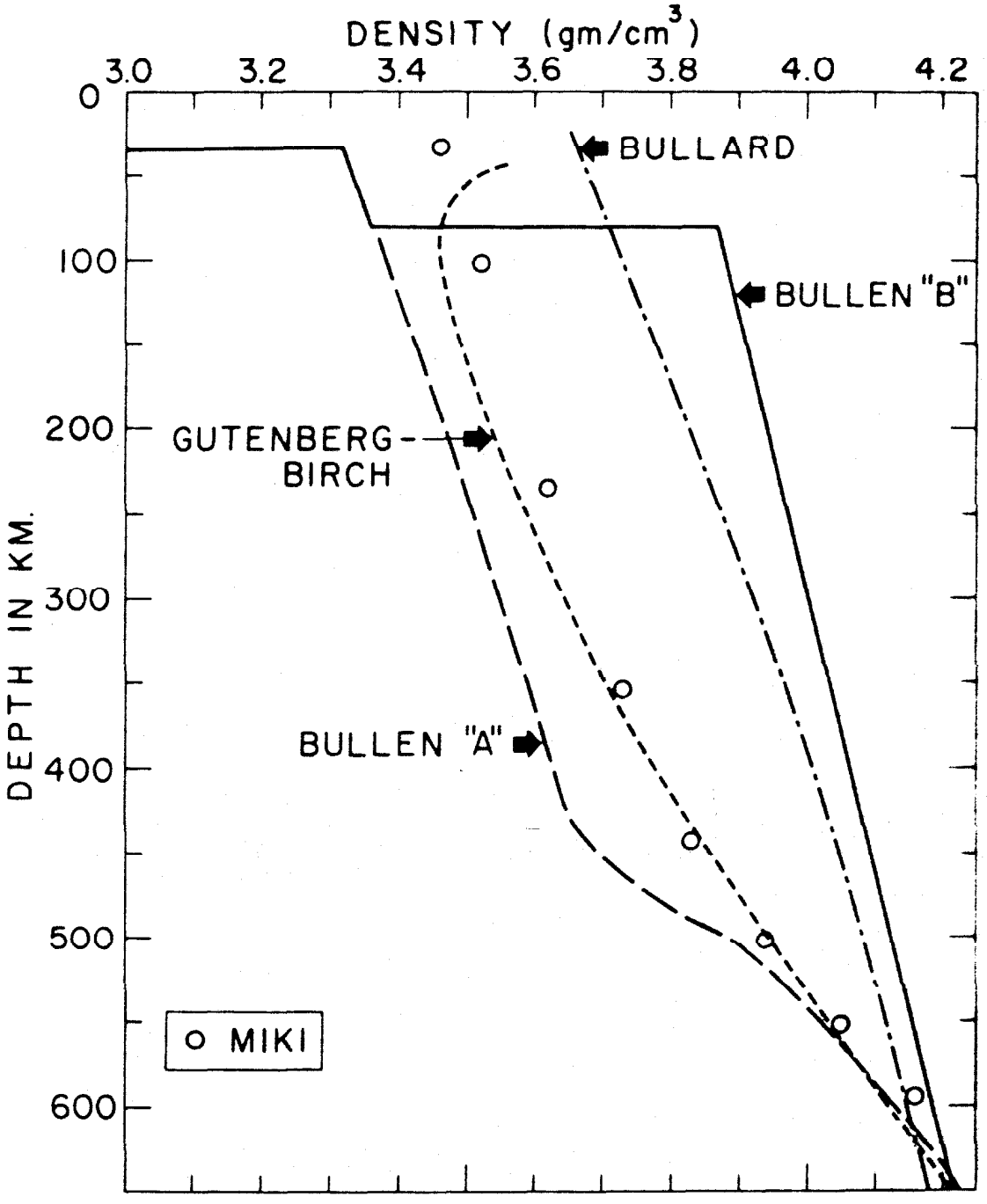
DENSITY (gm/cm³)
3.0
3.2
3.4
3.6
3.8
4.0
4.2
0
100
200
300
400
500
600
DEPTH IN KM.
BULLARD
BULLEN "B"
GUTENBERG-
BIRCH
BULLEN "A"
MIKI

FIG. 16

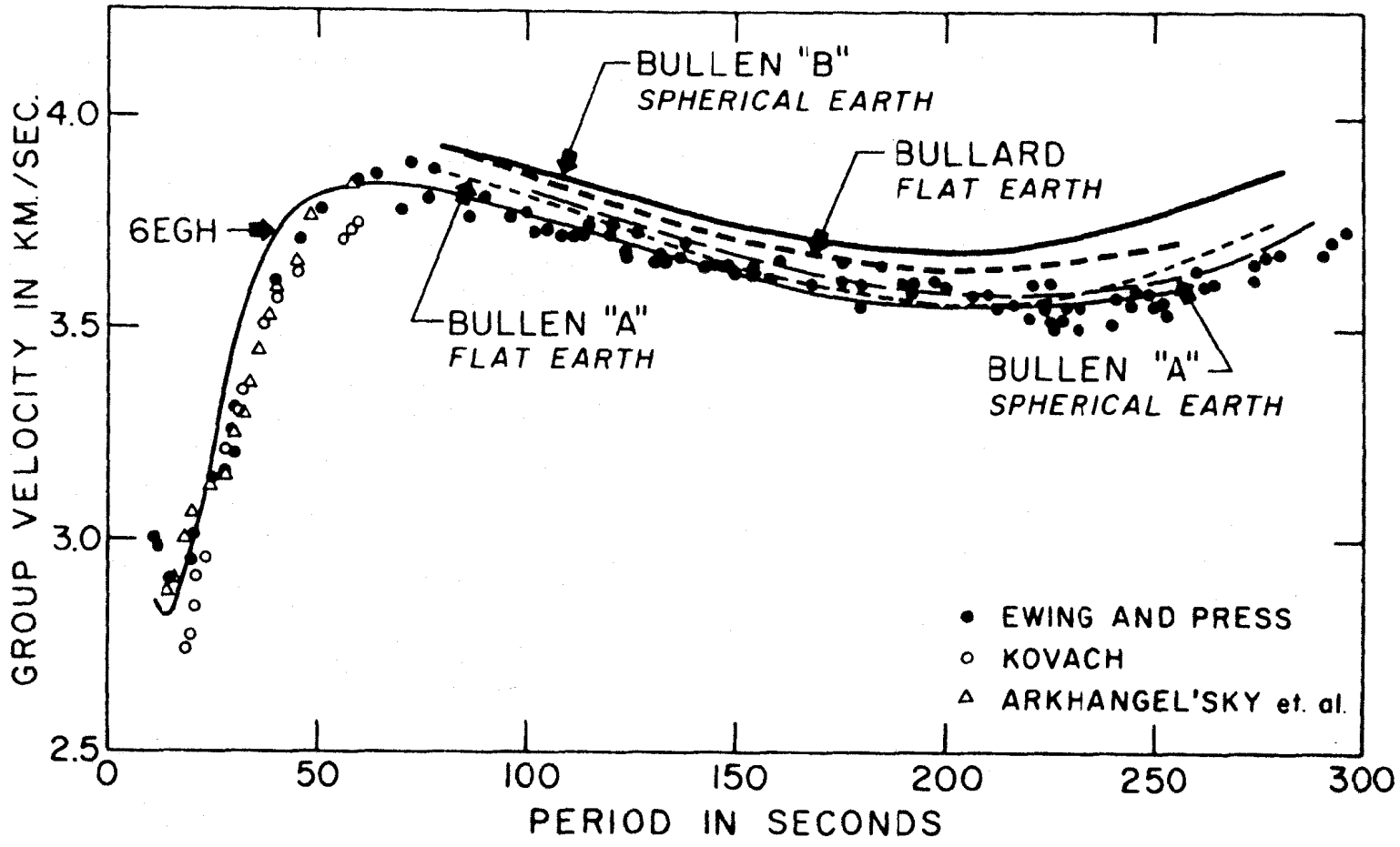
BULLEN "B"
SPHERICAL EARTH
BULLARD
FLAT EARTH
6EGH
BULLEN "A"
FLAT EARTH
BULLEN "A"
SPHERICAL EARTH
EWING AND PRESS
KOVACH
ARKHANGEL'SKY et. al.
GROUP VELOCITY IN KM./SEC.
4.0
3.5
3.0
2.5
0
50
100
150
200
250
300
PERIOD IN SECONDS

FIG. 17

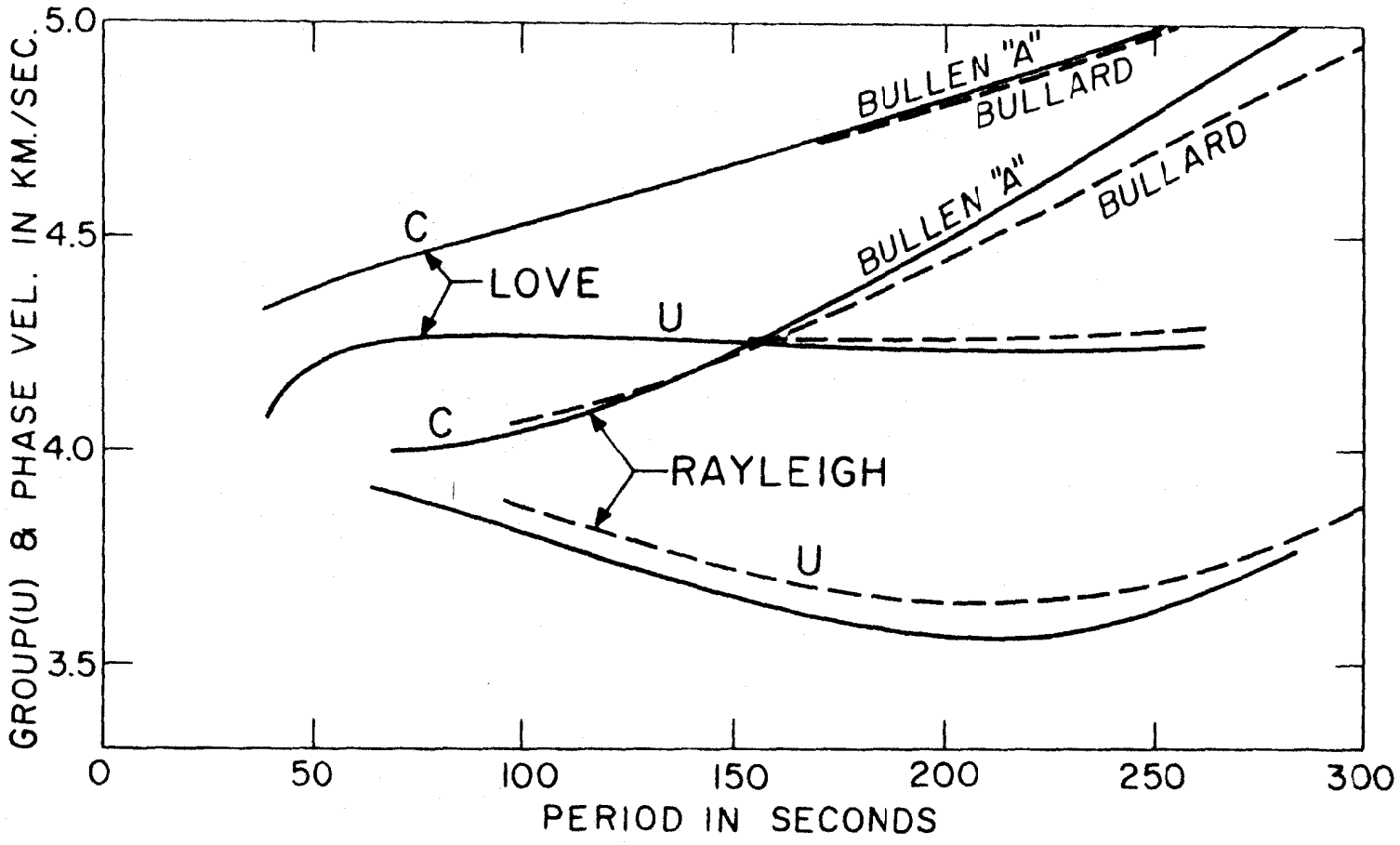
GROUP(U) & PHASE VEL. IN KM./SEC.
5.0
4.5
4.0
3.5
0
50
100
150
200
250
300
PERIOD IN SECONDS
BULLEN "A"
BULLARD
BULLEN "A"
BULLARD
C
LOVE
U
C
RAYLEIGH
U

FIG. 18

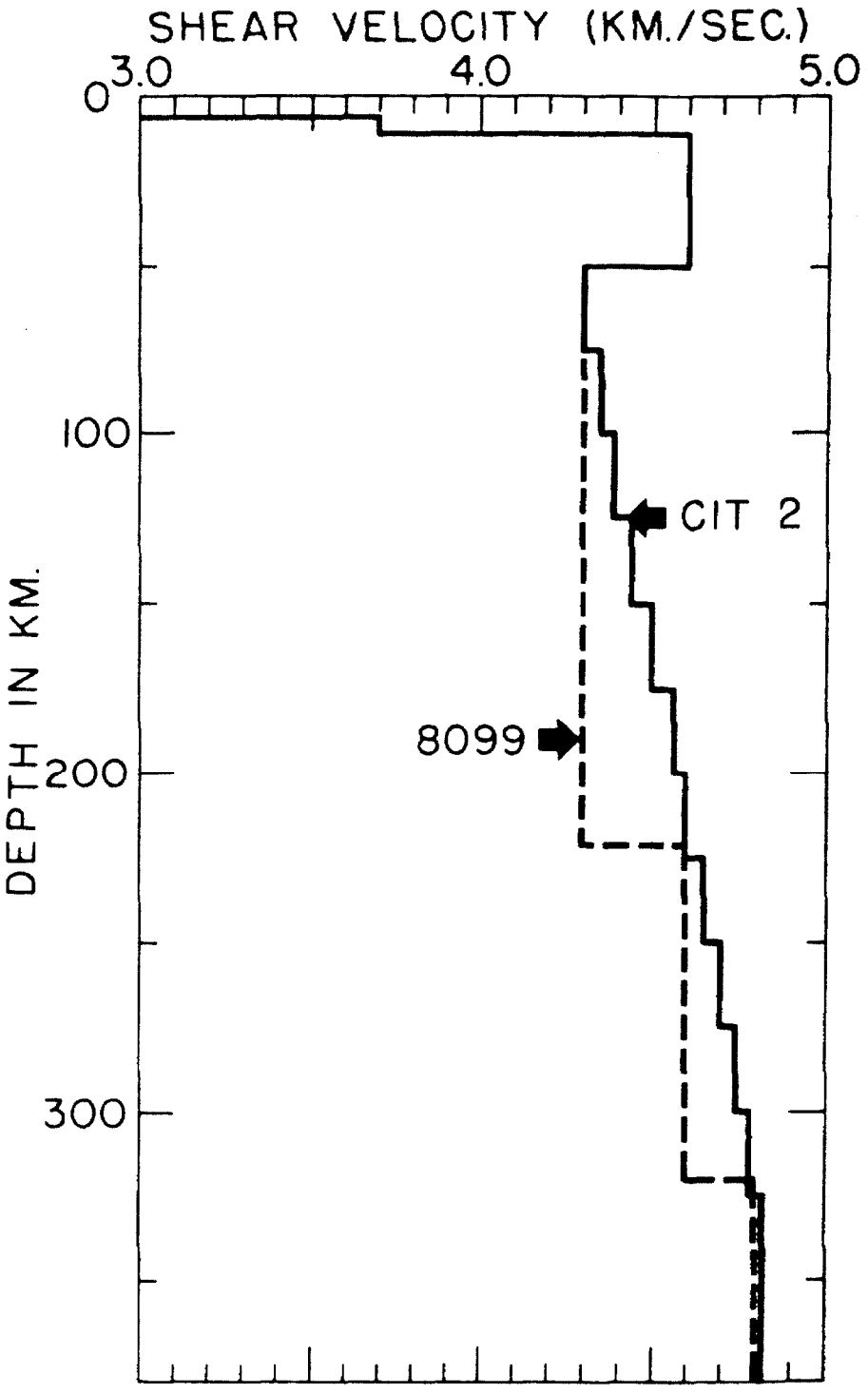
SHEAR VELOCITY (KM./SEC.)
3.0
4.0
5.0
0
100
200
300
DEPTH IN KM.
CIT 2
8099

FIG. 19

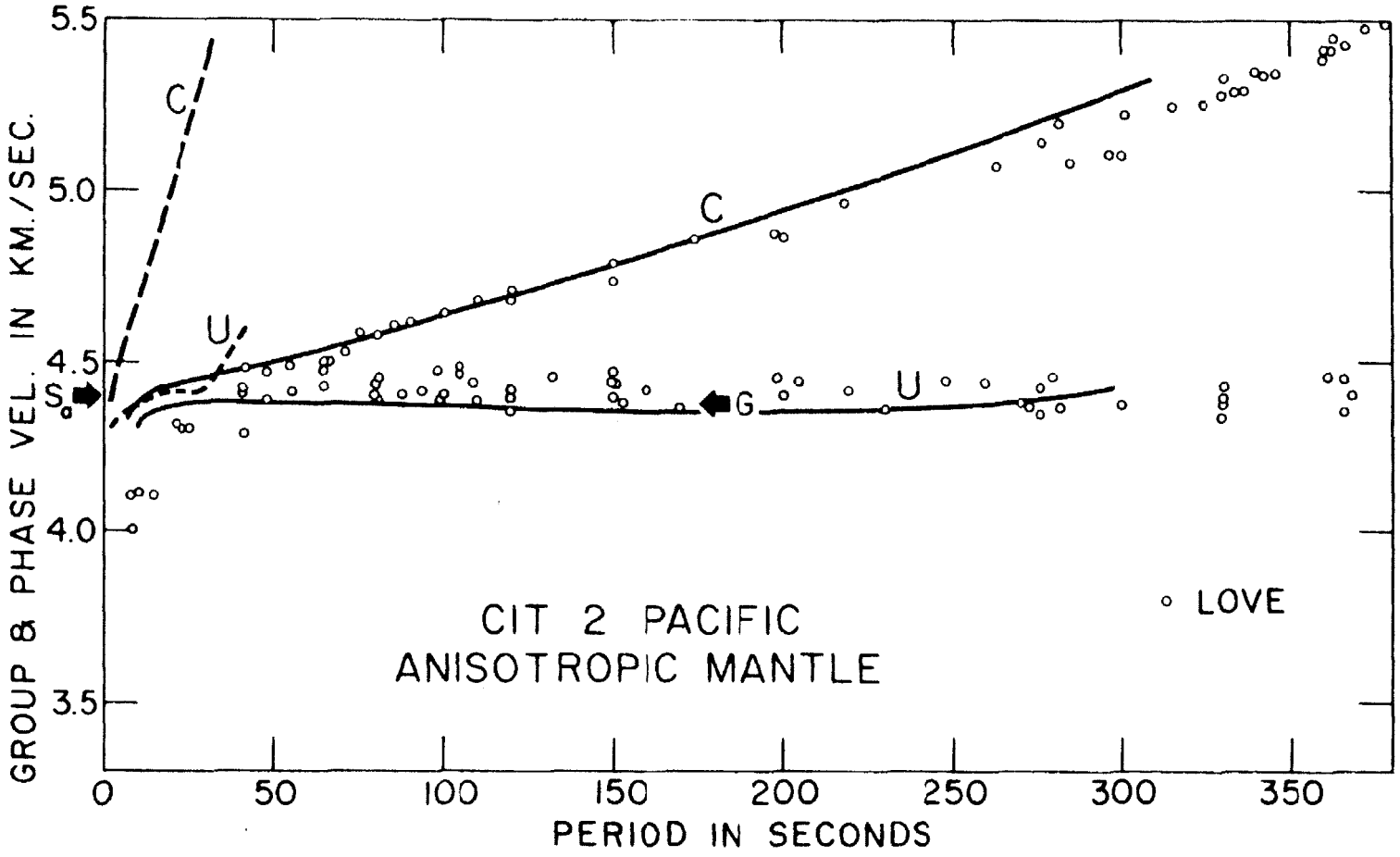
5.5
5.0
4.5
4.0
3.5
GROUP & PHASE VEL. IN KM./SEC.
C
C
U
U
G
S
CIT 2 PACIFIC
ANISOTROPIC MANTLE
LOVE
0
50
100
150
200
250
300
350
PERIOD IN SECONDS

FIG. 20

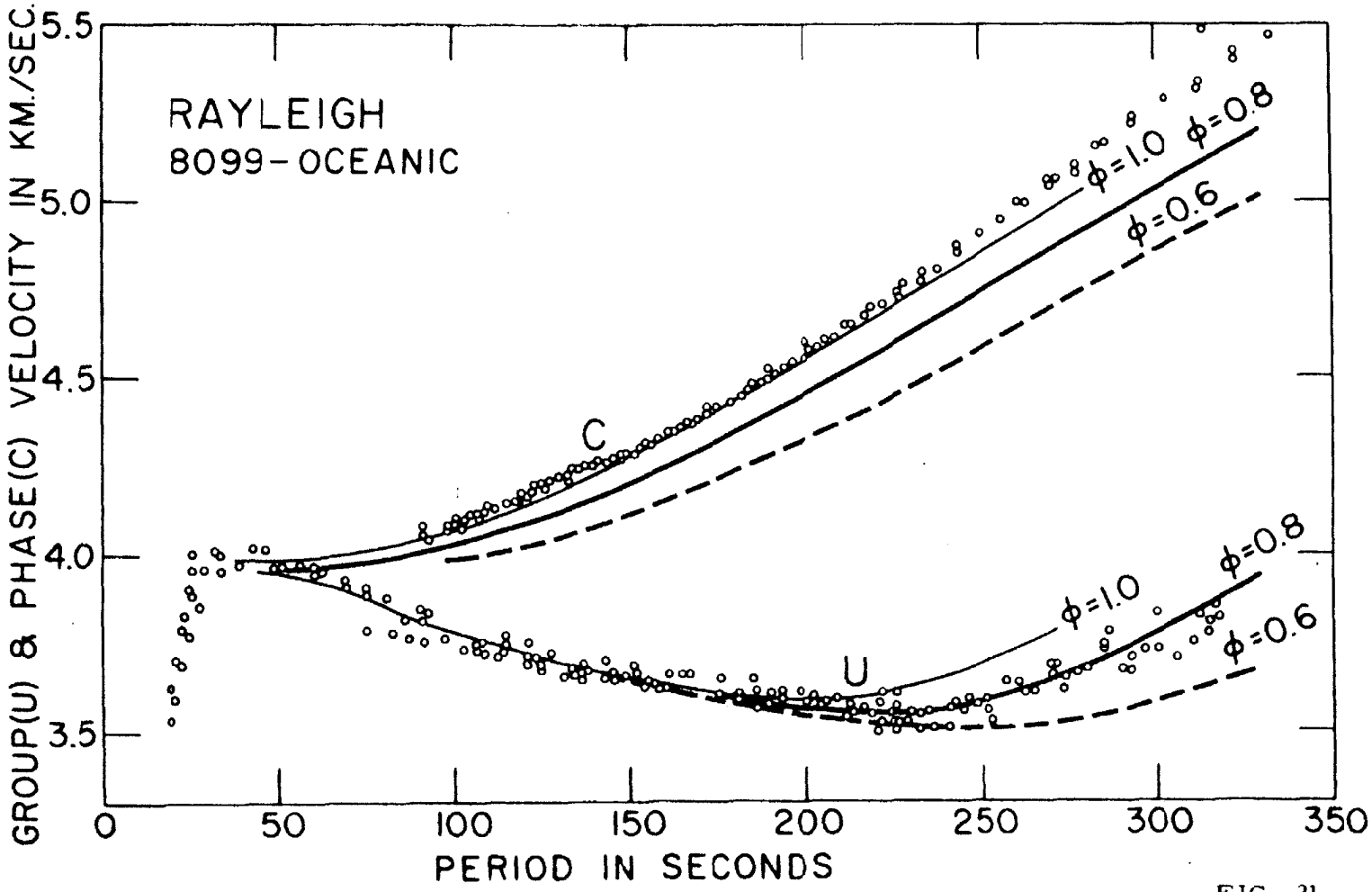
RAYLEIGH
8099-OCEANIC
GROUP(U) & PHASE(C) VELOCITY IN KM./SEC.
PERIOD IN SECONDS
C
U
φ=1.0
φ=0.8
φ=0.6
φ=1.0
φ=0.8
φ=0.6
5.5
5.0
4.5
4.0
3.5
0
50
100
150
200
250
300
350

FIG. 21